

General Disclaimer

One or more of the Following Statements may affect this Document

- This document has been reproduced from the best copy furnished by the organizational source. It is being released in the interest of making available as much information as possible.
- This document may contain data, which exceeds the sheet parameters. It was furnished in this condition by the organizational source and is the best copy available.
- This document may contain tone-on-tone or color graphs, charts and/or pictures, which have been reproduced in black and white.
- This document is paginated as submitted by the original source.
- Portions of this document are not fully legible due to the historical nature of some of the material. However, it is the best reproduction available from the original submission.

GO REPORT NO. 13

GRAVITY GRADIENT PRELIMINARY INVESTIGATIONS
FINAL REPORT ON EXHIBIT "B"
CONTRACT NAS 9-9200

PART I
FIELD GRAVITY SURVEY

PART II
LUNAR MASCON GRAVITY GRADIENTS

January 31, 1970

Prepared for

NATIONAL AERONAUTICS AND SPACE ADMINISTRATION
MANNED SPACECRAFT CENTER

Houston, Texas 77058

By

Lloyd G. D. Thompson
Mark H. Houston
Daniel A. Rankin



FACILITY FORM 602

| | |
|--|------------------|
| N70-20901 (ACCESSION NUMBER) | 1 (THRU) |
| 99 (PAGES) | 13 (CODE) |
| CR-108294 (NASA CR OR TMX OR AD NUMBER) | 13 (CATEGORY) |



General Oceanology, Inc.
27 Moulton Street
Cambridge, Mass. 02138
A Subsidiary of Bolt Beranek and Newman Inc

NASA CR 108294

GO REPORT NO. 13



General Oceanology, Inc., 27 Moulton St., Cambridge, Mass. 02138 • Tel. (617) 492-6300 • A Subsidiary of Bolt Beranek and Newman Inc.

GRAVITY GRADIENT PRELIMINARY INVESTIGATIONS

FINAL REPORT ON EXHIBIT "B"

CONTRACT NAS 9-9200

PART I

FIELD GRAVITY SURVEY

PART II

LUNAR MASCON GRAVITY GRADIENTS

January 31, 1970

Prepared for

NATIONAL AERONAUTICS AND SPACE ADMINISTRATION

MANNED SPACECRAFT CENTER

Houston, Texas 77058

By

Lloyd G. D. Thompson

Mark H. Houston

Daniel A. Rankin

FOREWARD

This report presents results of gravity and gravity gradient investigations performed under Exhibit "B" of the Statement of Work of Contract NAS 9-9200. Two separate items of work are covered in two independent parts of the report as follows:

- Part I - Field Gravity Survey
- Part II - Lunar Mascon Gravity Gradients

PART I
FIELD GRAVITY SURVEY

ABSTRACT

By a special surveying technique, horizontal gravity gradients as well as conventional gravity anomalies were obtained over a 5 km x 5 km area of the high desert south of Brothers, Oregon. Comparison of the two methods showed that the gradient technique appeared to be easier and more efficient both in data acquisition and data processing, but direct interpretation of the data was more difficult. Faulted basalt lava flows and a small rhyolite dome over a silicic vent, which are similar to features expected on the moon, gave gravity anomalies of 2 to 5 mgals and 0.85 mgals respectively. Vertical gravity gradients calculated from the gravity anomalies will provide reference and control values for future tests with a vertical gravity gradiometer.

TABLE OF CONTENTS

| <u>Section</u> | <u>Title</u> | <u>Page</u> |
|----------------|--|-------------|
| I | INTRODUCTION | 1 |
| II | SURVEY AREA | 3 |
| III | INSTRUMENTATION | 5 |
| IV | FIELD PROCEDURES | 7 |
| V | DATA REDUCTION AND PROCESSING | |
| | A. General | 11 |
| | B. Conventional Gravity Reduction | 11 |
| | C. Horizontal Gravity Gradient Reduction | 14 |
| VI | RESULTS | 17 |
| VII | INTERPRETATION | 36 |
| VIII | DISCUSSION | 38 |
| IX | CONCLUSIONS | 40 |
| X | RECOMMENDATIONS | 43 |
| | ACKNOWLEDGMENTS | 44 |
| | REFERENCES | 45 |

LIST OF ILLUSTRATIONS

| <u>Figure</u> | <u>Caption</u> | <u>Following Page</u> |
|---------------|---|-----------------------|
| 1 | Gravity meter operation at a typical field station showing the generally flat nature of the survey area | 4 |
| 2 | Fault Scarp looking Northwest from base station B-3 | 4 |
| 3 | Silicic vent looking Northeast from station S-5 with engineer's level in the foreground | 4 |
| 4 | Bench Mark at base station B-4 looking Northeast | 10 |
| 5 | Precise leveling operation at station S-17 looking Southeast | 10 |
| 6 | Topographic map of survey area showing gravity station locations | 16 |
| 7 | Free-Air gravity anomaly map | 35 |
| 8 | Bouguer gravity anomaly map | 35 |
| 9 | Residual anomaly map | 35 |
| 10 | Residual horizontal gradient map | 35 |
| 11 | Map of residual gravity anomalies and horizontal gradients for traverses over silicic vent | 35 |
| 12 | Residual gravity anomaly and horizontal gradient profiles over silicic vent | 35 |
| 13 | Interpretive model of silicic vent | 37 |

LIST OF TABLES

| <u>Table</u> | <u>Title</u> | <u>Page</u> |
|--------------|--|-------------|
| 1 | Principal Facts for Gravity Stations | 21 |
| 2 | Relative Gravity Anomaly Data | 23 |
| 3 | Horizontal Gradient Data | 29 |
| 4 | Average Horizontal Gradients over Sillicic Vent | 33 |
| 5 | Rock Sample Densities | 35 |

PART II
LUNAR MASCON GRAVITY GRADIENTS

ABSTRACT

A preliminary assessment illustrates the application and usefulness of gravity gradients for the detection and interpretation of lunar Mascons (mass concentrations or anomalies). Horizontal and vertical gradient profiles calculated from the lunar Bouguer anomaly map of O'Keefe give the gradient anomaly magnitudes and characteristic signatures over the Mascons of Mares Imbrium and Serenitatis. The horizontal gradient profiles vary through a range of as large as 35 Eotvos Units and the vertical gradient profiles through 50 Eotvos Units. Comparison of the Mascon gravity and gravity gradient signatures with those for simple geologic models shows that the Mascons are most probably near-surface disc- or plate-like structures of varying thickness. For more quantitative interpretation, more accurate gravity data or actual gradient measurements are required.

TABLE OF CONTENTS

| <u>Section</u> | <u>Title</u> | <u>Page</u> |
|----------------|--|-------------|
| I | INTRODUCTION | 47 |
| II | GRAVITY GRADIENT TECHNIQUES | 48 |
| III | APPLICATION OF GRADIENT TECHNIQUES TO LUNAR MASCONS | |
| | A. Lunar Gravity Data | 57 |
| | B. Methods of Gradient Calculation | 58 |
| IV | RESULTS | 62 |
| V | MASCON INTERPRETATIONS | 75 |
| VI | CONCLUSIONS | 77 |
| VII | RECOMMENDATIONS | 78 |
| | ACKNOWLEDGMENTS | 79 |
| | REFERENCES | 80 |
| APPENDIX A | A METHOD FOR COMPUTING THE GRAVITY AND GRAVITY GRADIENT ANOMALIES FOR TWO-DIMENSIONAL POLYGONS | 83 |
| APPENDIX B | DETERMINATION OF THE GRAVITY AND GRAVITY GRADIENT ANOMALIES OVER A VERTICAL CYLINDER | 89 |

LIST OF ILLUSTRATIONS

| <u>Figure</u> | <u>Caption</u> | <u>Page</u> |
|---------------|--|-------------|
| 1 | Normalized profiles of gravity anomaly, vertical gradient and horizontal gradient over a sphere centered beneath the origin | 50 |
| 2 | Normalized profiles of gravity anomaly, vertical gradient and horizontal gradient over a semi-infinite horizontal cylinder centered beneath the origin | 52 |
| 3 | Normalized profiles of gravity anomaly, vertical gradient and horizontal gradient over a semi-infinite fault | 53 |
| 4 | Normalized profiles of vertical gravity anomaly and vertical gradient over a flat plate | 56 |
| 5 | Bouguer anomaly map of the moon after O'Keefe (1968) | 59 |
| 6 | North-South gravity anomaly profile across Mare Imbrium | 63 |
| 7 | East-West gravity anomaly profile across Mare Imbrium | 64 |
| 8 | East-West gravity anomaly profile across Mare Serenitatis | 65 |
| 9 | North-South gravity anomaly profile across Mare Serenitatis | 66 |
| 10 | North-South horizontal gradient profile across Mare Imbrium | 67 |
| 11 | East-West horizontal gradient profile across Mare Imbrium | 68 |

LIST OF ILLUSTRATIONS (Cont.)

| <u>Figure</u> | <u>Caption</u> | <u>Page</u> |
|---------------|---|-------------|
| 12 | East-West horizontal gradient profile across Mare Serenitatis | 69 |
| 13 | North-South horizontal gradient profile across Mare Serenitatis | 70 |
| 14 | North-South vertical gradient profile across Mare Imbrium | 71 |
| 15 | East-West vertical gradient profile across Mare Imbrium | 72 |
| 16 | East-West vertical gradient profile across Mare Serenitatis | 73 |
| 17 | North-South vertical gradient profile across Mare Serenitatis | 74 |

LIST OF TABLES

| <u>Table</u> | <u>Title</u> | <u>Page</u> |
|--------------|--|-------------|
| 1 | Equations for gravity and gravity gradient anomalies for simple models | 49 |
| 2 | Comparison of characteristics of gradient signatures for simple models | 54 |

I. INTRODUCTION

This report covers the results of gravity field investigations performed under Exhibit "B" of the Statement of Work of Contract NAS 9-9200 in August and September, 1969.

A special purpose gravity survey was made over an area roughly 5 km on a side in the central Oregon desert. There were three primary objectives to the survey and subsequent data reduction:

1. To investigate and compare the ease of acquisition and usefulness of gravity, horizontal gravity gradient^{*}, and vertical gravity gradient^{**} data.
2. To investigate gravity and gravity gradient anomalies associated with lunar-like features.
3. To support other geophysical investigations being done in the area by the Manned Spacecraft Center (MSC), NASA, Houston, Texas and the University of Oregon (under contract with NASA, MSC).

* Rate of change of the vertical component of gravity in the horizontal direction.

** Rate of change of the vertical component of gravity in the vertical direction.

There has been some investigation of the possible usefulness of gravity gradient techniques. The vertical gradient seems to hold considerable promise for the detailed resolution of near surface features (Thompson, Houston and Rankin, 1969), especially if suitable instrumentation can be developed to measure this gradient directly. The possible use of horizontal gradients has been previously investigated (Thyssen-Bornemisza and Stackler, 1962a, 1962b; Thyssen-Bornemisza, 1965). Among the attractive features of these gradient methods is the relative simplicity of data acquisition and reduction.

Certain features of the moon, the Mascons in particular, show peculiar large gravity anomalies (Muller and Sjogren, 1968). The area surveyed in this study has been formed by magmatic flows, intrusives and faulting and, in general, contains structures which might bear a resemblance to lunar features. Therefore, a careful study of the gravity field over these known features might aid in the interpretation of lunar structures.

The Geophysics Branch, MSC, Houston, and the University of Oregon are undertaking a broad geophysical survey program of this region of Oregon. This program includes monitoring of ambient seismic noise, micro-earthquake studies, magnetic surveys, local and regional gravity surveys. This General Oceanology study is a part of that overall program.

II. SURVEY AREA

The survey area was chosen in consultation with sponsoring NASA officials and University of Oregon scientists. The physical features in the area have been formed by magmatic activity and may bear some resemblance to features on the moon. The area lies in the region being investigated by the MSC seismic program with a NASA Mobile Geophysical Laboratory and the University of Oregon.

The survey site is a square roughly 5 km on a side, located in central Oregon on U.S. Highway 20 with the little town of Brothers at the northeast corner. The "Brothers Fault Zone", a NW-SE trending zone of faults which stretches across central Oregon, passes through the area. The area is a relatively flat high desert (about 4,700 feet above sea level). It is part of the immense Columbia Basalt Plateau, a feature composed of several thousand feet of magmatic flows which have been deposited over a vast area of Oregon, Washington and Idaho during and since the Tertiary period. Some of the most recent flows are hardly more than 1,000 years old, for example, as seen at Craters of the Moon National Monument in Idaho.

The survey site as shown on the U.S. Geological Survey Reconnaissance Geological Map (Walker, Peterson and Greene, 1967), has surface basalt of Tertiary and Quaternary ages overlying late Tertiary basalt. The surface is covered with a soft mixture of loose weathered volcanic ash several feet deep.

The survey area is generally flat as can be seen in Figure 1 but it contains two prominent physical features. One is a vertical fault escarpment which trends east-west in the lower middle of the area and is shown in part in Figure 2. The surface expression of

of the fault extends for several kilometers. The maximum relief is perhaps 10 meters. The rock outcrop of the fault scarp is dense, solid basalt formed in several layers or flows. The other feature is a dome of extrusive rock over a silicic vent near the middle of the area which is shown in Figure 3. In profile from afar the vent appears as an almost symmetrical mound with a shape much like the rounded head of a rivet or carriage bolt. The total vertical relief from plain to the top of the hill is approximately 30 meters. The material composing the dome, as sampled by a pit dug midway up the northern slope, is a reddish, light weight rhyolite.



Figure 1. Gravity meter operation at a typical field station showing the generally flat nature of the survey area.



Figure 2. Fault Scarp looking Northwest from base station B-3.

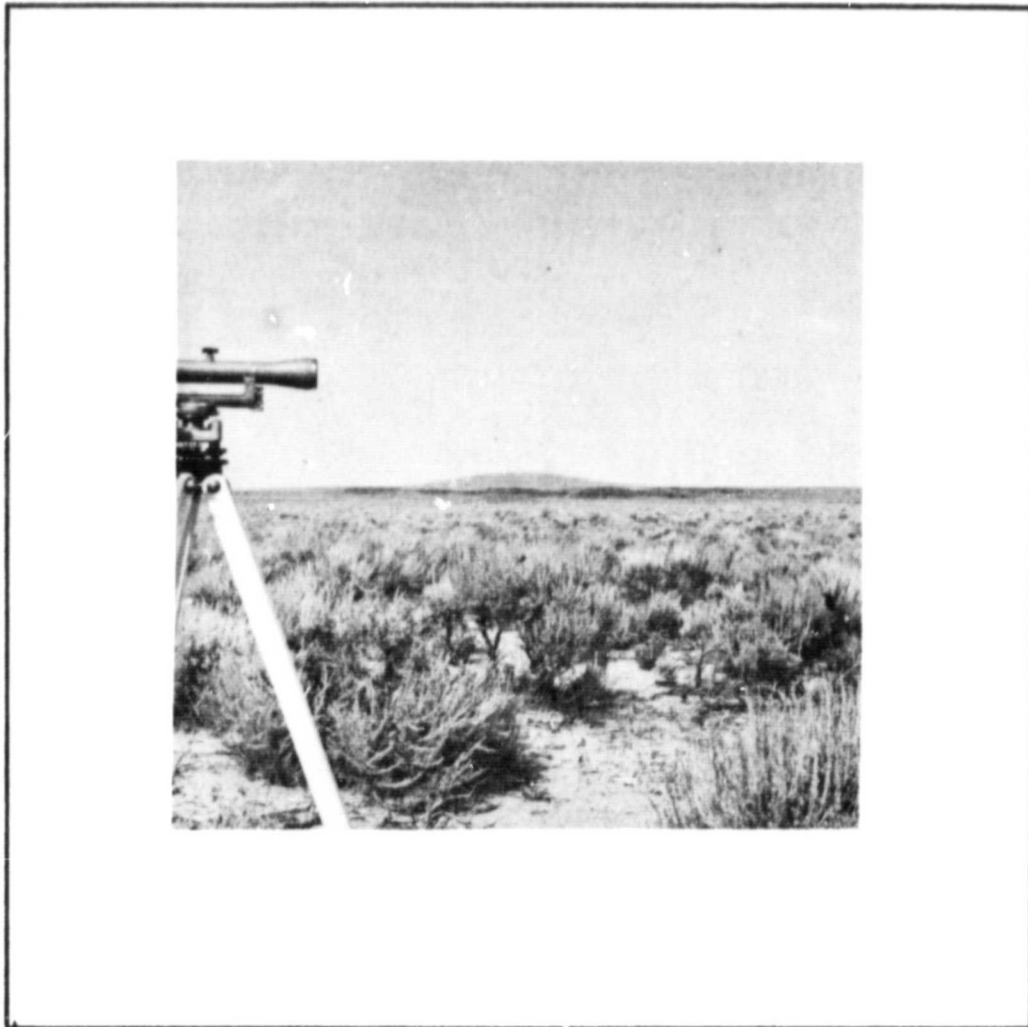


Figure 3. Silicic vent looking Northeast
from station S-5 with engineer's
level in the foreground.

III. INSTRUMENTATION

The survey was carried out using two North American gravity meters serial numbers #7 and #93. They have a history of excellent performance with extremely low drift rates and good repeatability. They also have low calibration constants which make them particularly suitable for precision gravity surveys.

The calibration of the two meters was checked by a series of measurements on a portion of the University of Oregon calibration line which runs from the campus in Eugene, Oregon to the rim of Crater Lake, Oregon (Blank and Barnes, unpublished manuscript). The calibration constants for the meters was found to be in excellent agreement with values from former calibrations. Specifically, the calibration constants used for this work were 0.08938 mgal*/div. for #7 and 0.09102 mgal/div. for #93.

With these gravity meters the dial setting can be accurately read by means of a vernier scale to one tenth of a scale division. An experienced operator can make gravity measurements which will repeat within ± 1 or at most ± 2 tenths of scale division which corresponds to about ± 0.01 or ± 0.02 mgal.

One of the requirements of a gravity survey is the determination of station locations and precise elevations. This was accomplished using a Brunton-type compass for azimuth or direction, a Gurley Engineer's level and rod for precise levelling, and a 100 ft. surveyors chain for measuring distances.

* Earth's Normal Gravity Acceleration is about 980 cm/sec^2 ;
 $1 \text{ cm/sec}^2 = 1 \text{ gal}$; $1 \text{ milligal (mgal)} = 1 \times 10^{-3} \text{ gal} = 1 \times 10^{-3} \text{ cm/sec}^2$;
 $1 \text{ Eotvos Unit} = 1 \times 10^{-9} \text{ gal/cm} = 1 \times 10^{-9} \text{ l/sec}^2$.

The field equipment, gravity meters with their attendant batteries, and personnel were carried in a station wagon. The rear baggage compartment was modified to accept a pair of padded buckets which held the gravity meters. The batteries, which are connected to the gravity meters at all times to supply power for internal temperature stabilization heaters and internal lights, were secured in the station wagon and connected in parallel to the station wagon's battery. This arrangement proved very satisfactory.

The automobile was driven to all but a very few gravity measurement sites. The gravity meter power cables were approximately five meters long, allowing the meters to be transferred from the station wagon to the tripod stand without interruption of power. A portable battery was connected to the meter the few times it was impossible to drive directly to the gravity measuring site.

IV. FIELD PROCEDURES

Gravity measurements were made at selected points within the survey area which were positioned in such a way as to yield a variety of data. The main reference point for the survey was near Bench Mark H373 at a location which was identified as base B-1. To obtain the area-wide gravity data, measurements were made at seven other Bench Marks (stations B-2 through B-8) similar to the Bench Mark shown in Figure 4 and eighteen landmark locations (stations S-1 through S-18) whose elevations were given on the local topographic map (Brothers Quadrangle, 1967).

Horizontal gravity gradients were obtained by taking gravity readings at substation locations around each "B" or "S" gravity station. At least two and sometimes four substations were laid out, using the compass and chain, in N-S-E-W directions to allow computation of two horizontal gradient components from which a total horizontal gradient vector could be obtained. The substations were 300 ft. from the base station. In two cases, B-2 and S-9, it was not feasible to make substation measurements. These substations and their directional location relative to the base station are identified by a letter N,S,E,W, after the base station's name.

In addition, a third major pattern of stations was established consisting of a set of crossed double profiles over the rhyolite dome. This network of stations allowed the construction of gravity profiles and horizontal gradient profiles over the dome.

Gravity measurements, as obtained by a gravimeter, are relative measurements of the gravity at one point compared to that at another point. Values of the true or total gravity can be obtained only by connecting the reference point of the local survey

to some point having a known gravity value. Such a point of known gravity related to the world datum exists at the town of Hampton, Oregon (Rinehart, Bowen, and Chiburis, 1964). This was used as a reference gravity value and the main base for the survey was connected to it by double looping.*

It was convenient, during the course of the survey, to set up a number of reference stations to minimize driving time and instrument drift. The primary base station was B-1 and all reference stations were at least double-looped to it.

The field procedure was straightforward. Sites for measurements were selected from the topographic map by consideration of access, known elevations and desire for uniform coverage of the area. At the site, the Bench Mark or point of known elevation would be located. Depending on the characteristics of the location, the site for the gravity reading would be taken directly at the Mark or a few feet from it. The levelling tripod and Brunton-type compass would be set up directly over this main reading site. The compass and chain were then used to lay out the horizontal substations 300 ft. from the base in N-S-E-W directions. Either two or four substations would be located.

The station wagon was then driven to the main station location and a gravity reading obtained as shown in Figure 1. The level was set up at some convenient spot and used, with the rod, to determine the elevation of the gravity meter tripod ring relative to the point of known elevation as shown in Figures 3 and 5. The car was then driven to the substations and similar gravity and elevation readings determined. As a final check,

* A technique of making repeated readings at two stations to eliminate errors from gravity meter drift and diurnal gravity tide effects.

closing readings were again taken at the main station. Typically, a complete station with layout, levelling, and gravity readings would require two to four hours with three persons working.

The stations for the detailed profiles over the rhyolite dome were laid out, then levelled, and finally occupied with the gravity meter. The layout started from the top of the hill. Lines were run north, south, and east with stations marked at 100, 300, 500, 1000, 1500, 2000, and 2500 ft. from the origin. To the west locations were marked to 500 ft. From each station on the N-S line, except within 500 ft. of the origin, a point was laid out 300 ft. to the east. On the W-E line, a point was laid out 300 ft. north of each station 500 or more feet from the origin.

Elevations were run in with the rod and level from Bench Mark M22 (location B-3) and closed at station S-14 as a check. It was found that the top of the hill is approximately 3 feet lower than the elevation given on the topographic map (the elevation at S-14 agreed with the map value). On a relative basis, we believe our elevations of the profile stations are correct and of sufficiently high order of accuracy.

The station wagon was driven to all but a few locations on the hill. At the exceptions, the gravimeter was connected to a portable battery and carried to the measurement site.

Samples of the basalt which composes the structure of the plain were obtained from the exposure caused by the fault. Except for slight surface weathering, this rock was very solid, so solid in fact that it was hard to obtain samples. The surface layer was somewhat vesicular but the deeper layers were more massive and solid.

The rock of the silicic vent was sampled from a pit which had been dug about midway up the northern slope of the hill. This material was a light, reddish, fine-grained rhyolite.

An attempt to measure earth tides at the location of the NASA seismic van was planned. However, lack of time and personnel at the van precluded such measurements.



Figure 4. Bench Mark at base station B-4
looking Northeast.

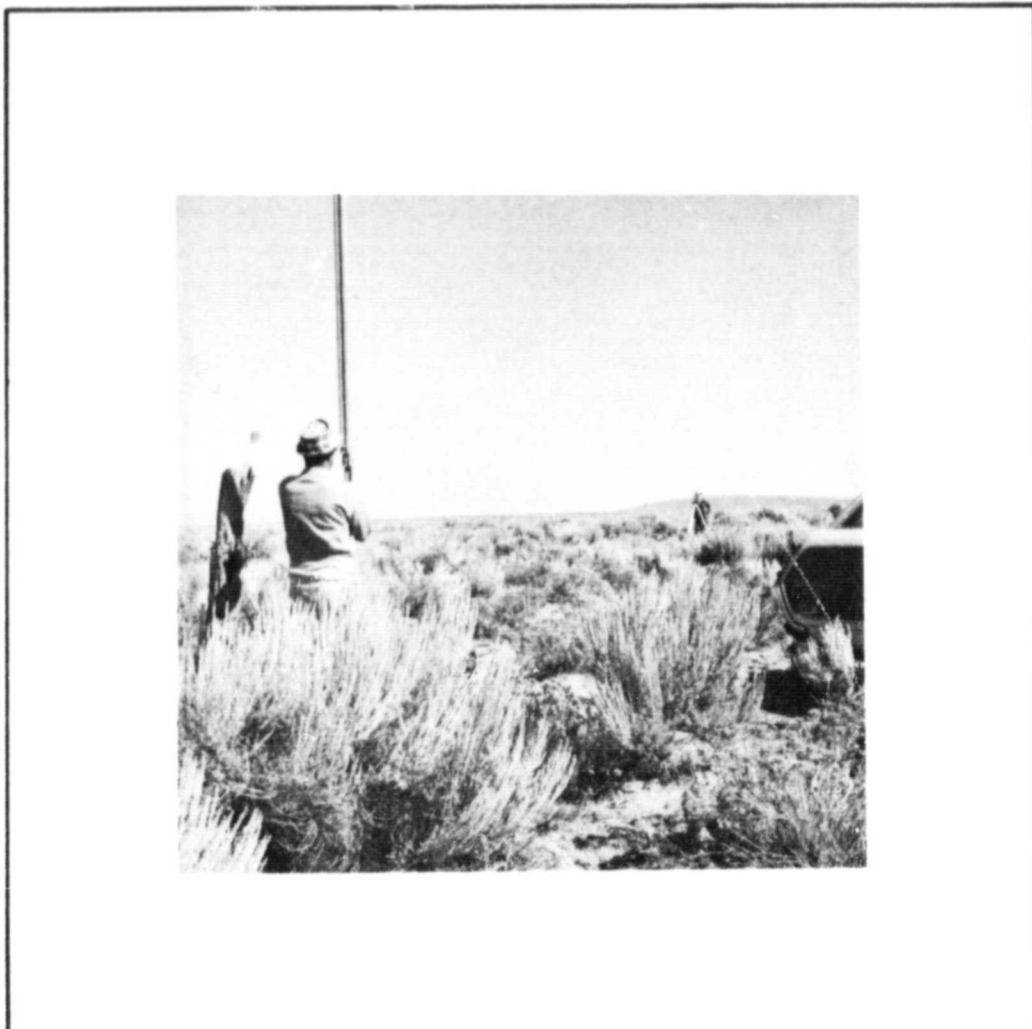


Figure 5. Precise leveling operation at station S-17 looking Southeast.

V. DATA REDUCTION AND PROCESSING

A. GENERAL

Gravity measurements were made at 118 points within the survey area. A map of the station locations is given in Figure 6. The field data were reduced in two ways to yield two types of information. The first was conventional reduction to gravity Principle Facts and anomalies. The other was reduction to horizontal gravity gradients.

B. CONVENTIONAL GRAVITY REDUCTION

Several textbooks on geophysical exploration (cf. Dobrin, 1960; Grant and West, 1965) and innumerable survey reports detail the necessary corrections and conventional method of reduction of gravity data. First, it is necessary to convert the instrument readings at the various stations into gravity differences relative to a reference base. Then a series of corrections must be applied to the gravity differences to remove all known causes of gravity variation except subsurface density variations.

Each station reading is made at some time on a loop between readings at the main base or some auxiliary base. To correct for changes in instrument readings due to gravity tides or instrument drift, the readings are plotted on time-base graph paper and a proper value for the base reading at the time of the station reading is found. The corrected base reading is then subtracted from the station reading to yield a corrected difference measured in gravity meter dial divisions. When this is multiplied by the gravity meter calibration constant, the difference in gravity is obtained.

There are a series of corrections which must be made to these values before they become comparable. A Free-Air correction of 0.09406 mgal/ft. is made to adjust for the decrease in gravity with increasing elevation. This correction is added for stations above the reference plane and subtracted for stations below the reference plane. The Bouguer correction is required to adjust for the rock mass between the elevation of measurement and the elevation to which the Free-Air correction is made. This factor has the value $0.01276 \times (\text{density of material in gm/cm}^3)$ mgal/ft. In this particular case, a density of 2.75 was used, which meant a Bouguer correction of 0.3509 mgal/ft. This correction is subtracted for stations above the reference plane and added for those below. A latitude correction is necessary to correct for the systematic increase in the value of gravity from the equator to either pole. The value of this correction changes with latitude. By a standard formula, the correction at the latitude of our survey is 2.474×10^{-4} mgal/ft. This correction is added for stations south of the reference and subtracted for those to the north. At some stations surrounded by rough terrain, it may be necessary to make a terrain correction for deviations from a plane ground surface in the neighborhood of the point. After these corrections are made, it may be necessary or desirable to make a regional correction to remove any overall slope in the gravity field over the survey area so that local features will stand out more clearly.

The object of all these corrections is to remove all causes of change in the value of gravity except the internal mass distribution beneath the survey area.

There are several ways of reporting the results of gravity surveys. The "Principle Facts" are a tabulation of data which report station identification and location and certain gravity values and anomalies in terms which are directly comparable with

all other gravity data on a world-wide basis. The total or "absolute" value of gravity relative to the world datum at each point on the survey is reported together with the latitude, longitude, and elevation of the station. The Free-Air anomaly at sea level is also given which is determined by correcting the observed gravity value to sea level and subtracting a spheroid gravity value computed from the International Gravity Formula:

$$g(\phi) = 978.0490 (1 + 0.0052884 \sin^2\phi - 0.0000059 \sin^2 2\phi) \text{ cm/sec}^2 ,$$

where ϕ equals the station latitude. The Bouguer anomaly referenced to sea level is computed by the same technique as above except that the Bouguer correction for the intervening mass is also made using a conventional density of 2.67 gms/cm^3 .

The precision and accuracy of the Principle Facts is not too high for they cannot be any better than the accuracy of the known "absolute" gravity at the reference point and the accuracy of the station elevations. Within a local survey itself, the relative accuracies are much better.

The local data, relative to itself, is reported in three forms: Free-Air anomalies, Bouguer anomalies, and residual anomalies. The Free-Air anomalies are computed, each station relative to the base, with only latitude and elevation (Free-Air) corrections to the raw gravity difference data. The Bouguer anomalies include Free-Air, Bouguer, latitude and terrain corrections. The residual anomalies are computed after a Bouguer anomaly map has been plotted to determine the direction and magnitude of any persistent regional slope in the data, and removing that slope by a final correction.

In order to make all of these corrections, it is necessary to have very accurate information for the location and elevation of the stations. If one assumes the gravity meter can make readings accurate to 0.01 milligal and demands similar precision in the corrections, then elevations must be known to within about 0.1 ft. and north-south positions to within about 40 ft. On many gravity surveys, the efforts involved in levelling and locating the stations exceeds the effort of taking the actual gravity readings.

C. HORIZONTAL GRAVITY GRADIENT REDUCTION

The horizontal gravity gradients were obtained by the simple procedure of dividing the gravity difference from slightly separated stations by the horizontal distance between the stations. At 23 locations, patterns of stations were laid out and gravity readings taken to allow such computations. At all but two of the "B" and "S" locations at least two and sometimes four substations were occupied 300 ft. from the main station. Any two stations will allow computation of the component of the horizontal gradient between them. Computation of the total horizontal gradient, however, requires knowledge of two components, measured at right angles. The five-station pattern probably yields a better average value but involves more work and if used exclusively, would have resulted in reduction in the total number of horizontal gradient determinations within the survey area.

The gravity meter reading differences between the substations and main station are determined, then converted to gravity differences by multiplication by the gravity meter calibration factor. The Free-Air and Bouguer corrections are applied to the substations relative to the main station. The latitude correction is applied to any north-south substations. In areas

of very uneven local terrain, it may be necessary to make a terrain correction to the substations relative to the main station. With these simple corrections one obtains the change in gravity with horizontal distance associated with local unknown masses. Division of these changes by the horizontal distance yields horizontal gradient components. With two such components at right angles one can determine the magnitude and azimuth of the total horizontal vector.

The horizontal gradients are expressed in terms of Eotvos Units (see footnote page 5; 1 E.U. = 10^{-9} cm/sec²/cm). Over a 300 ft. horizontal span, a gravity difference of 0.01 mgal is approximately equivalent to a gradient of one E.U.

It if is discovered that there is a persistent gravity gradient in the survey area, it may be desirable to remove it in order to emphasize local features. This is easily accomplished, at least to a first order linear slope, by averaging all of the north-south gradient components and correcting each station for any mean value. The same should be done for the east-west components. The resulting vectors, when recomputed from the corrected components, will show no area-wide directional bias.

In the gradient technique, each cluster of stations yields a gradient vector which is independent of measurements tying the cluster to any base reference. There is no need for area-wide levelling as only the relative elevations within each cluster are needed. Looping with the gravity meter is required only within each cluster, rather than having all readings made relative to a fixed base. The surveying within the cluster must be reasonably accurate, meaning that levelling should be within 0.1 ft. and horizontal distances within 5 ft. The location of the clusters relative to each other need be known only as well as the mapmaker

demands. This will be a function of the density of stations, the magnitude and dimensional size of the anomaly, and intent of the survey.

In this particular survey, a double traverse was made over the rhyolite dome in the N-S and W-E directions. This produced a ladder-like pattern of stations. As suggested by Thyssen-Bornemiza (1965), the horizontal gradients were determined at the mid-points of the rectangles of the ladder. This was accomplished by taking the average of the east-west gradients on the top (north) and bottom (south) sides of each box as the proper east-west gradient in the middle of the box. A similar procedure was used for the north-south component. Thus, the double traverse produced a single, but averaged, gradient profile.

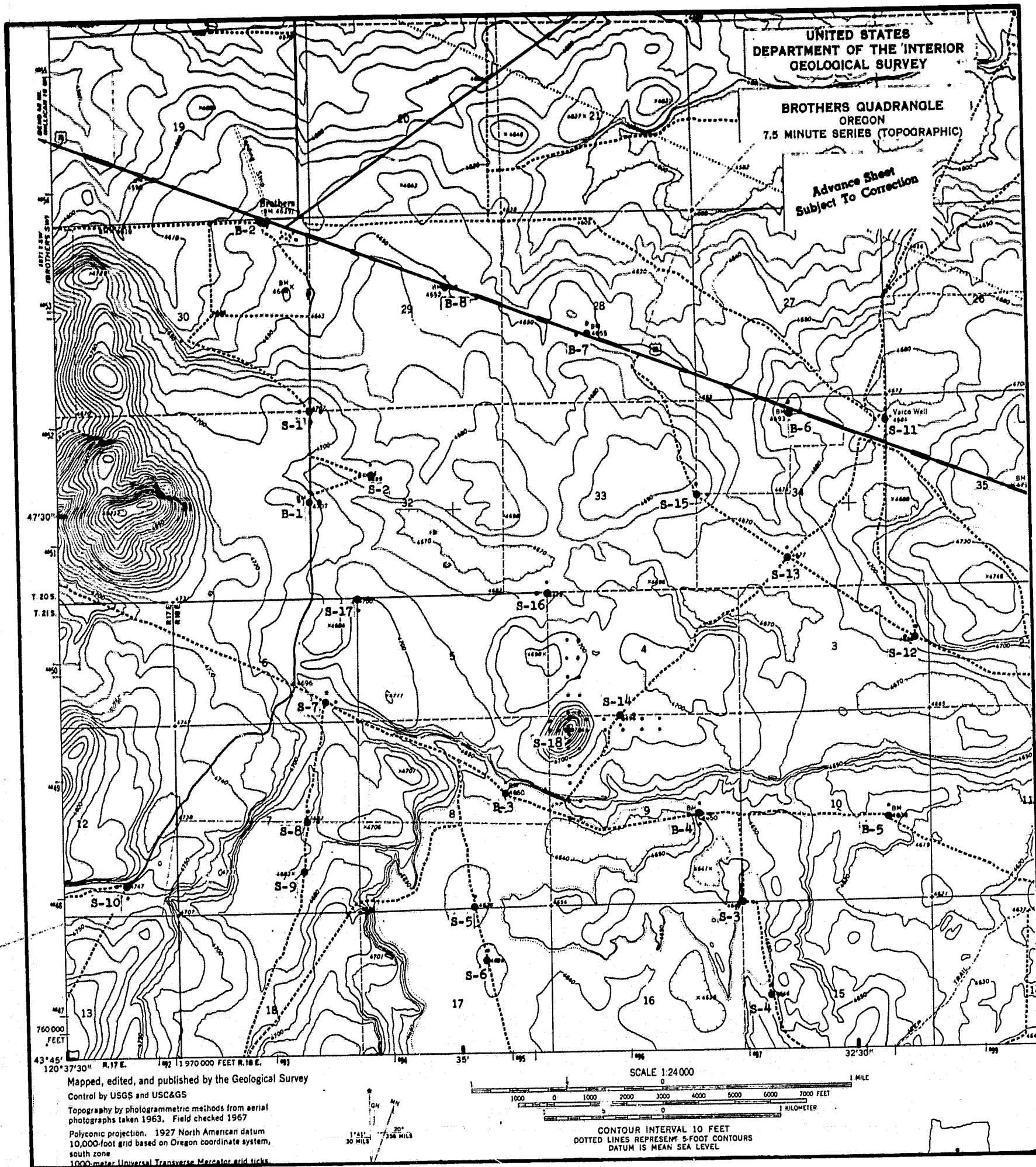


Figure 6. Topographic map of survey area showing gravity station locations.

VI. RESULTS

The Principle Facts for all gravity stations are given in Table 1. The gravity values are relative to the base station value of 980.0951 gals at the Hampton Airport which was previously established on the World Datum by Rinehart et al (1964).

The Free-Air, Bouguer, and residual anomalies for all stations relative to the main base B-1 are tabulated in Table 2. The Free-Air anomaly map of the area is shown in Figure 7. Since most of the area is topographically flat, this map generally reflects the density variations beneath the surface except for the areas of the fault scarp and the dome of the silicic vent where the effect of topography is noted.

The Bouguer anomaly map of the area is shown in Figure 8. This shows that a pronounced north-trending gradient exists in this area.

After removing this strong regional gradient, the residual anomaly map is shown in Figure 9. It is noted that the added stations at 300 ft. intervals give more control on the position of the contours. In this case, with a station spacing of about 1 km, the contouring is relatively easy and definitive although the anomaly pattern is general in nature. The residual anomalies are not totally enclosed within the survey area but occur at the perimeter of the survey area as alternate highs and lows radiating outwards from the silicic vent. The residual anomalies vary in magnitude from 2 to 5 mgals and the anomaly over the rhyolite dome is about 0.85 mgals.

The horizontal gradients calculated from the residual gravity values are given in Table 3. A map of the residual horizontal gradients (corrected for the strong regional north gradient) is given in Figure 10. The pattern of gradient vectors pointing to areas of greater rock density is readily noted. Areas of high and low density can be inferred and are indicated on Figure 10. These correspond to the areas of high and low gravity anomalies in Figure 9. However, a method of the direct interpretation or outlining of the high or low density areas (which can be done with gravity anomaly values) from a map of gradient vectors is not developed as yet.

The average horizontal gradients derived from parallel traverses over the rhyolite dome are given in Table 4. The residual anomalies for the profile stations are given in Table 2. A plot of the residual anomaly values and the residual average horizontal gradients for the traverses over the hill is shown in Figure 11. The gravity anomaly values show variations along the profiles but with a limited number and distribution of stations not much can be told of the horizontal distribution of anomaly causing masses. The horizontal gradients, however, not only provide profiles of gradient magnitude but also indicate the presence of and direction to higher density anomaly masses. The path of injection of the lighter rhyolite of the silicic vent and the presence of the rhyolite plug itself are inferred in Figure 11.

The gravity anomaly profiles along the two north-south lines and the base east-west line are shown in Figure 12 together with a profile of the magnitudes of the horizontal gradients resolved in a north-south direction. A negative gravity anomaly of about 0.85 milligals is shown over the rhyolite dome which reflects the density contrast of about 0.5 gms/cc between the basalt lava flows and the rhyolite. The horizontal gradient curve is approximately

the derivative of the mean gravity anomaly curve and shows a peak-to-peak variation of about 60 E.U. as it passes over the dome (the horizontal gradient passes through zero over the center of a three-dimensional body). The effect of the fault at about 1,700 ft. south is barely noticeable on the gravity anomaly profile but it is distinctly detected by the horizontal gradient anomaly (the horizontal gradient reaches a maximum over the edge of a fault).

Vertical gravity gradient values have been calculated for a number of key points throughout the survey area and are shown on the residual anomaly map in Figure 9. There are several approximation methods for calculating vertical gradients from a gravity anomaly map. After investigating these various methods, one following Grant and West (1965) was found to be most suitable for this particular case. In this method the vertical gradient U_{zz} is approximated by the equation:

$$U_{zz} = \frac{U_{z_0}}{r_0} + \sum_{i=1}^N \overline{U_{z_i}} \left[\frac{1}{r_{i-1}} - \frac{1}{r_i} \right],$$

where r_0 is the radius of a small finite circle around the calculation point over which the gravity anomaly is essentially constant, U_{z_0} is the gravity anomaly at the calculation point, and $\overline{U_{z_i}}$ is the average gravity anomaly in the ring between radius r_{i-1} and radius r_i . The equation is evaluated with the aid of a template sectioned into convenient divisions of radius and angle which permits determination of $\overline{U_{z_i}}$ for different rings. The selection of appropriate ring radii for the extent and wavelength of the gravity anomalies being used is important to give a close approximation to the true gradient. Tests of this method using simple sphere and flat plate models showed that the estimated vertical gradients were always within 10% of the true gradients.

In view of the star-shaped or radial pattern of the gravity anomalies shown in Figure 9, no completely enclosed anomaly is available within the area to provide the opportunity to calculate optimum vertical gradients (for example, at the center of a high). The vertical gradient values appear, however, to be of correct order of magnitude and variation for the anomaly pattern. The calculation points were selected to give approximate sections across the survey area. Vertical gradient profiles across the vent are dominated by the intense negative gradient value over the vent itself but, if plotted, do reflect a typical vertical gradient anomaly curve for this anomaly pattern.

The densities of different samples of rhyolite from the silicic vent and from various phases of basalt flows exposed on the fault scarp are given in Table 5. The density of the rhyolite is more or less constant at about 2.24 gms/cc while the basalt varies from about 2.64 gms/cc to 2.75 gms/cc. The mean density of the basalt samples is 2.70 gms/cc. From observation of the fault scarp, it appeared that the vesicular phases existed chiefly nearer the surface while the deeper flows were more solid in nature. Thus it was felt that the density of the underlying basalt flows, which govern the anomaly pattern, would more likely have a density of 2.75 gms/cc. This was, therefore, the density used in calculating the Bouguer corrections. Also, the density contrast between the rhyolite and basalt was taken to be 0.50 gms/cc.

TABLE 1 - PRINCIPAL FACTS FOR GRAVITY STATIONS

| NO. | NAME | LATITUDE | | LONGITUDE | ELEVATION FEET | OBS GRAVITY GALS | GRAVITY ANOMALIES | |
|-----|---|----------|------|-----------|-------------------|---------------------|-------------------|------------------|
| | | ° | ' | | | | FREE AIR MGALS | BOUGUER MGALS |
| B-1 | BM H373 | 43 | 47.5 | 120 | 4706 | 980.1086 | 18.6 | -141.7 |
| B-2 | Brothers (at site of destroyed B.M.) | | 48.6 | 36.2 | 4640 | .1173 | 19.1 | -138.9 |
| B-3 | BM M22 | | 46.2 | 34.7 | 4651 | .1014 | 8.3 | -150.1 |
| B-4 | BM J373 | | 46.1 | 33.5 | 4651 | .0997 | 6.7 | -151.7 |
| B-5 | BM K373 | | 46.0 | 32.3 | 4639 | .0988 | 5.0 | -153.0 |
| B-6 | BM B373 | | 47.9 | 32.9 | 4694 | .1090 | 13.1 | -145.2 |
| B-7 | BM No. 36(1929) State Hwy. Dept. | | 48.3 | 34.1 | 4656 | .1121 | 16.3 | -142.3 |
| B-8 | BM Z372 | | 48.5 | 35.0 | 4653 | .1134 | 17.0 | -141.5 |
| S-1 | | | 48.0 | 35.9 | 4708 | .1096 | 19.2 | -141.1 |
| S-2 | | | 47.7 | 35.5 | 4700 | .1080 | 17.2 | -142.9 |
| S-3 | | | 45.7 | 33.2 | 4644 | .0972 | 4.2 | -154.0 |
| S-4 | | | 45.2 | 33.0 | 4647 | .0960 | 4.0 | -154.3 |
| S-5 | | | 45.7 | 34.9 | 4639 | .0991 | 5.6 | -152.4 |
| S-6 | | | 45.4 | 34.8 | 4639 | .0979 | 4.8 | -153.2 |

TABLE 1 (Cont.) - PRINCIPAL FACTS FOR GRAVITY STATIONS

| NO. | NAME | LATITUDE | | LONGITUDE | ELEVATION FEET | OBS GRAVITY GALS | GRAVITY ANOMALIES | | |
|------|------------|----------|------|-----------|-------------------|---------------------|-------------------|------------------|--------|
| | | ° | ' | | | | FREE AIR MGALS | BOUGUER MGALS | |
| S-7 | | 43 | 46.6 | 120 | 35.8 | 4685 | 980.1025 | 11.9 | -147.7 |
| S-8 | | | 46.1 | | 36.0 | 4683 | .0991 | 9.2 | -150.3 |
| S-9 | | | 45.9 | | 36.0 | 4682 | .0972 | 7.5 | -151.9 |
| S-10 | | | 45.8 | | 37.1 | 4748 | .0924 | 8.9 | -152.8 |
| S-11 | Varco Well | | 47.9 | | 32.3 | 4684 | .1108 | 18.3 | -141.3 |
| S-12 | | | 46.9 | | 32.1 | 4697 | .1022 | 12.4 | -147.6 |
| S-13 | | | 47.2 | | 32.9 | 4678 | .1062 | 14.0 | -145.3 |
| S-14 | | | 46.5 | | 34.0 | 4697 | .1006 | 11.3 | -148.7 |
| S-15 | | | 47.6 | | 33.5 | 4691 | .1073 | 15.9 | -143.9 |
| S-16 | | | 47.1 | | 34.4 | 4677 | .1049 | 12.8 | -146.5 |
| S-17 | | | 47.1 | | 35.6 | 4701 | .1053 | 15.5 | -144.6 |
| S-18 | Hilltop | | 46.5 | | 34.3 | 4781 | .0940 | 12.7 | -150.2 |

TABLE 2 - RELATIVE GRAVITY ANOMALY DATA

| STATION | LOCATION re: B-1 FT. | | ELEVATION ABOVE MSL FEET | ANOMALIES re: B-1 MGALS | | |
|---------|----------------------|--------------|--------------------------------|-------------------------|---------|----------|
| | N-S + = N | E-W + = E | | FREE AIR | BOUGUER | RESIDUAL |
| B-1 | 0 | 0 | 4706.11 | 0.00 | 0.02 | 0.02 |
| N | 300 | 0 | 4699.42 | - 0.34 | - 0.08 | -0.33 |
| S | - 300 | 0 | 4708.08 | - 0.50 | - 0.41 | -0.16 |
| E | 0 | 300 | 4700.25 | - 0.50 | - 0.28 | -0.28 |
| W | 0 | - 300 | 4713.34 | 0.89 | 0.66 | 0.66 |
| B-2 | 7925 | -1225 | 4640.30 | 0.54 | 2.87 | -3.80 |
| B-3 | - 8250 | 5300 | 4650.83 | -10.36 | - 8.41 | -1.47 |
| N | - 7950 | 5300 | 4659.26 | -10.05 | - 8.39 | -1.70 |
| E | - 8250 | 5600 | 4643.46 | -10.59 | - 8.38 | -1.44 |
| B-4 | - 8925 | 10675 | 4650.90 | -11.89 | - 9.96 | -2.45 |
| N | - 8625 | 10675 | 4648.24 | -11.32 | - 9.29 | -2.04 |
| S | - 9225 | 10675 | 4650.26 | -12.31 | -10.35 | -2.59 |
| E | - 8925 | 10975 | 4647.74 | -11.99 | - 9.94 | -2.43 |
| W | - 8925 | 10375 | 4644.68 | -11.80 | - 9.64 | -2.13 |
| B-5 | - 9125 | 15950 | 4638.85 | -13.83 | -11.47 | -3.79 |
| N | - 8825 | 15950 | 4635.04 | -13.74 | -11.25 | -3.83 |
| E | - 9125 | 16250 | 4632.42 | -14.57 | -11.99 | -4.31 |
| B-6 | 2175 | 13375 | 4693.85 | - 1.29 | - 0.84 | -2.67 |
| N | 2475 | 13375 | 4693.68 | - 0.96 | - 0.50 | -2.58 |
| E | 2175 | 13675 | 4690.83 | - 1.14 | - 0.58 | -2.41 |

TABLE 2 (Cont.) - RELATIVE GRAVITY ANOMALY DATA

| STATION | LOCATION re: B-1 FT. | | ELEVATION ABOVE MSL FEET | ANOMALIES re: B-1 MGALS | | |
|---------|----------------------|--------------|--------------------------------|-------------------------|---------|----------|
| | N-S + = N | E-W + = E | | FREE AIR | BOUGUER | RESIDUAL |
| B-7 | 4525 | 7825 | 4655.54 | - 2.34 | - 0.56 | -4.37 |
| N | 4825 | 7825 | 4652.82 | - 2.64 | - 0.77 | -4.83 |
| W | 4525 | 7525 | 4655.05 | - 2.67 | - 0.88 | -4.69 |
| B-8 | 5925 | 3900 | 4652.99 | - 1.62 | 0.22 | -4.76 |
| N | 6225 | 3900 | 4651.75 | - 1.56 | 0.35 | -4.89 |
| E | 5925 | 4200 | 4646.19 | - 2.21 | - 0.10 | -5.08 |
| S-1 | 2550 | 25 | 4708.48 | 0.64 | 0.58 | -1.56 |
| N | 2850 | 25 | 4705.27 | 0.66 | 0.71 | -1.69 |
| S | 2250 | 25 | 4711.07 | 0.59 | 0.43 | -1.46 |
| E | 2550 | 325 | 4707.19 | 0.34 | 0.32 | -1.82 |
| W | 2550 | - 275 | 4706.94 | 0.99 | 0.98 | -1.16 |
| S-2 | 700 | 1750 | 4700.43 | - 1.33 | - 1.13 | -1.72 |
| N | 1000 | 1750 | 4696.22 | - 1.44 | - 1.08 | -1.92 |
| W | 700 | 1450 | 4699.20 | - 0.94 | - 0.69 | -1.28 |
| S-3 | -11250 | 11950 | 4643.91 | -14.42 | -12.24 | -2.78 |
| N | -10950 | 11950 | 4643.19 | -14.26 | -12.05 | -2.84 |
| E | -11250 | 12250 | 4641.60 | -14.49 | -12.22 | -2.76 |
| S-4 | -14050 | 12625 | 4647.35 | -14.59 | -12.52 | -0.70 |
| N | -13750 | 12625 | 4649.56 | -14.45 | -12.46 | -0.89 |
| E | -14050 | 12925 | 4652.15 | -14.39 | -12.49 | -0.67 |

TABLE 2 (Cont.) - RELATIVE GRAVITY ANOMALY DATA

| STATION | LOCATION re: B-1 FT. | | ELEVATION ABOVE MSL FEET | ANOMALIES re: B-1 MGALS | | |
|---------|----------------------|--------------|--------------------------------|-------------------------|---------|----------|
| | N-S + = N | E-W + = E | | FREE AIR | BOUGUER | RESIDUAL |
| S-5 | -11225 | 4400 | 4639.43 | -12.98 | -10.64 | -1.20 |
| N | -10925 | 4400 | 4639.60 | -12.92 | -10.58 | -1.39 |
| E | -11225 | 4700 | 4639.33 | -12.93 | -10.59 | -1.15 |
| S-6 | -12950 | 4725 | 4639.38 | -13.81 | -11.45 | -0.56 |
| N | -12650 | 4725 | 4639.07 | -13.60 | -11.24 | -0.60 |
| E | -12950 | 5025 | 4638.84 | -13.89 | -11.53 | -0.64 |
| S-7 | - 5625 | 375 | 4685.41 | - 6.67 | - 5.93 | -1.20 |
| N | - 5325 | 375 | 4685.86 | - 6.67 | - 5.95 | -1.47 |
| E | - 5625 | 675 | 4685.30 | - 6.91 | - 6.17 | -1.44 |
| S-8 | - 8925 | - 225 | 4683.43 | - 9.38 | - 8.58 | -1.07 |
| N | - 8625 | - 225 | 4683.36 | - 8.89 | - 8.08 | -0.83 |
| E | - 8925 | 75 | 4694.94 | - 9.33 | - 8.93 | -1.42 |
| S-9 | -10275 | - 350 | 4682.00 | -11.08 | -10.22 | -1.58 |
| S-10 | -10625 | -5275 | 4748.26 | - 9.65 | -11.08 | -2.14 |
| S | -10925 | -5275 | 4739.26 | -10.21 | -11.34 | -2.15 |
| W | -10625 | -5575 | 4743.68 | - 9.65 | -10.92 | -1.98 |
| S-11 | 2000 | 16025 | 4684.04 | - 0.35 | 0.43 | -1.25 |
| N | 2300 | 16025 | 4676.72 | - 0.33 | 0.70 | -1.23 |
| W | 2000 | 15745 | 4690.52 | - 0.11 | 0.44 | -1.24 |

TABLE 2 (Cont.) - RELATIVE GRAVITY ANOMALY DATA

| STATION | LOCATION re: B-1 FT. | | ELEVATION ABOVE MSL FEET | ANOMALIES re: B-1 MGALS | | RESIDUAL |
|---------|----------------------|--------------|--------------------------------|-------------------------|---------|----------|
| | N-S + = N | E-W + = E | | FREE AIR | BOUGUER | |
| S-12 | - 4150 | 16775 | 4697.37 | - 6.14 | - 5.83 | -2.36 |
| N | - 3850 | 16775 | 4698.56 | - 5.76 | - 5.49 | -2.25 |
| W | - 4150 | 16475 | 4692.57 | - 6.45 | - 5.97 | -2.50 |
| S-13 | - 1825 | 13250 | 4678.31 | - 4.59 | - 3.62 | -2.08 |
| N | - 1525 | 13250 | 4676.87 | - 4.21 | - 3.18 | -1.90 |
| E | - 1825 | 13550 | 4676.56 | - 4.54 | - 3.50 | -1.96 |
| S-14 | - 6175 | 8450 | 4697.00 | - 7.30 | - 6.98 | -1.79 |
| S | - 6475 | 8450 | 4696.82 | - 7.71 | - 7.38 | -1.93 |
| E | - 6175 | 8750 | 4696.88 | - 7.37 | - 7.04 | -1.85 |
| S-15 | - 25 | 10775 | 4690.55 | - 2.78 | - 2.23 | -2.21 |
| N | 275 | 10775 | 4690.36 | - 2.64 | - 2.08 | -2.31 |
| E | - 25 | 11075 | 4685.72 | - 2.94 | - 2.21 | -2.19 |
| S-16 | - 2650 | 6550 | 4677.19 | - 5.79 | - 4.78 | -2.55 |
| N | - 2350 | 6550 | 4674.59 | - 5.62 | - 4.52 | -2.54 |
| W | - 2650 | 6250 | 4678.15 | - 5.87 | - 4.89 | -2.66 |
| S-17 | - 2750 | 1300 | 4701.06 | - 3.09 | - 2.91 | -0.60 |
| S | - 3050 | 1300 | 4701.51 | - 3.45 | - 3.29 | -0.72 |
| E | - 2750 | 1600 | 4699.39 | - 3.34 | - 3.11 | -0.80 |
| S-18 | - 6525 | 7100 | 4781.46 | - 5.89 | - 8.21 | -2.72 |
| 25N | - 4025 | 7100 | 4701.46 | - 5.80 | - 5.63 | -2.24 |

TABLE 2 (Cont.) - RELATIVE GRAVITY ANOMALY DATA

| STATION | LOCATION re: B-1 FT. | | ELEVATION ABOVE MSL FEET | ANOMALIES re: B-1 MGALS | | |
|---------|----------------------|--------------|--------------------------------|-------------------------|---------|----------|
| | N-S + = N | E-W + = E | | FREE AIR | BOUGUER | RESIDUAL |
| 25N 3E | - 4025 | 7400 | 4701.45 | - 5.79 | - 5.62 | -2.23 |
| 20N | - 4525 | 7100 | 4696.36 | - 6.36 | - 6.01 | -2.20 |
| 20N 3E | - 4525 | 7400 | 4700.20 | - 5.99 | - 5.78 | -1.97 |
| 15N | - 5025 | 7100 | 4700.11 | - 6.38 | - 6.17 | -1.94 |
| 15N 3E | - 5025 | 7400 | 4699.35 | - 6.15 | - 5.91 | -1.68 |
| 10N | - 5525 | 7100 | 4695.28 | - 7.01 | - 6.62 | -1.97 |
| 10N 3E | - 5525 | 7400 | 4692.83 | - 6.97 | - 6.49 | -1.84 |
| 5N | - 6025 | 7100 | 4716.75 | - 7.11 | - 7.39 | -2.32 |
| 5N 3E | - 6025 | 7400 | 4716.52 | - 7.02 | - 7.32 | -2.25 |
| 3N | - 6225 | 7100 | 4749.97 | - 6.49 | - 7.82 | -2.58 |
| 1N | - 6425 | 7100 | 4777.74 | - 5.98 | - 8.14 | -2.74 |
| 1S | - 6625 | 7100 | 4777.86 | - 6.05 | - 8.25 | -2.67 |
| 3S | - 6825 | 7100 | 4759.42 | - 6.60 | - 8.24 | -2.50 |
| 5S | - 7025 | 7100 | 4735.59 | - 7.26 | - 8.16 | -2.25 |
| 5S 3E | - 7025 | 7400 | 4711.27 | - 8.50 | - 8.60 | -2.69 |
| 10S | - 7525 | 7100 | 4693.07 | - 9.01 | - 8.52 | -2.19 |
| 10S 3E | - 7525 | 7400 | 4685.80 | - 9.02 | - 8.31 | -1.98 |
| 15S | - 8025 | 7100 | 4679.30 | - 9.30 | - 8.35 | -1.60 |
| 15S 3E | - 8025 | 7400 | 4688.08 | - 9.04 | - 8.38 | -1.63 |

TABLE 2 (Cont.) - RELATIVE GRAVITY ANOMALY DATA

| STATION | LOCATION re: B-1 FT. | | ELEVATION ABOVE MSL FEET | ANOMALIES re: B-1 MGALS | | RESIDUAL |
|---------|----------------------|--------------|--------------------------------|-------------------------|---------|----------|
| | N-S + = N | E-W + = E | | FREE AIR | BOUGUER | |
| 20S | - 8525 | 7100 | 4666.21 | - 10.25 | - 8.81 | - 1.64 |
| 20S 3E | - 8525 | 7400 | 4669.07 | - 10.19 | - 8.87 | - 1.70 |
| 25S | - 9025 | 7100 | 4644.11 | - 10.99 | - 8.80 | - 1.21 |
| 25S 3E | - 9025 | 7400 | 4646.39 | - 10.94 | - 8.82 | - 1.23 |
| 5W | - 6525 | 6600 | 4721.19 | - 7.77 | - 8.21 | - 2.72 |
| 5W 3N | - 6225 | 6600 | 4704.48 | - 8.09 | - 8.00 | - 2.76 |
| 3W | - 6525 | 6800 | 4747.43 | - 6.84 | - 8.10 | - 2.61 |
| 1W | - 6525 | 7000 | 4776.89 | - 6.00 | - 8.18 | - 2.69 |
| 1E | - 6525 | 7200 | 4776.86 | - 6.03 | - 8.20 | - 2.71 |
| 3E | - 6525 | 7400 | 4753.08 | - 6.59 | - 8.11 | - 2.62 |
| 5E | - 6525 | 7600 | 4722.23 | - 7.49 | - 7.97 | - 2.48 |
| 5E 3N | - 6225 | 7600 | 4716.42 | - 7.12 | - 7.39 | - 2.15 |
| 10E | - 6525 | 8100 | 4690.18 | - 8.10 | - 7.51 | - 2.02 |
| 10E 3N | - 6225 | 8100 | 4691.31 | - 7.80 | - 7.25 | - 2.01 |
| 15E | - 6525 | 8600 | 4696.46 | - 7.78 | - 7.44 | - 1.95 |
| 15E 3N | - 6225 | 8600 | 4696.45 | - 7.41 | - 7.07 | - 1.83 |
| 20E | - 6525 | 9100 | 4694.43 | - 7.95 | - 7.54 | - 2.05 |
| 20E 3N | - 6225 | 9100 | 4695.91 | - 7.62 | - 7.26 | - 2.02 |
| 25E | - 6525 | 9600 | 4692.95 | - 8.28 | - 7.82 | - 2.33 |
| 25E 3N | - 6225 | 9600 | 4693.98 | - 7.88 | - 7.46 | - 2.22 |

TABLE 3 - HORIZONTAL GRADIENT DATA

| STATIONS BASE SUB | CORR. Δg MGALS | DISTANCE FEET | GRADIENT COMPONENTS EOTVOS UNITS | | THG | | RESIDUAL | |
|-------------------------|---------------------------|------------------|-------------------------------------|-----------------|-----|-----|----------|-----|
| | | | U _{xz} | U _{yz} | MAG | AZ | MAG | AZ |
| B-1 B-1N S E W | -0.10 | 300 | | -11 | 55 | 289 | 52 | 260 |
| | -0.43 | 300 | | 47 | | | | |
| | -0.30 | 300 | -33 | | | | | |
| | 0.64 | 300 | -70 | | | | | |
| B-3 B-3N E | 0.03 | 300 | 3 | 3 | 5 | 045 | 25 | 173 |
| | 0.03 | 300 | | | | | | |
| B-4 B-4N S E W | 0.67 | 300 | | 73 | 61 | 344 | 34 | 331 |
| | -0.40 | 300 | | 44 | | | | |
| | 0.01 | 300 | 1 | | | | | |
| | 0.31 | 300 | -34 | | | | | |
| B-5 B-5N E | 0.23 | 300 | | 25 | 62 | 294 | 57 | 266 |
| | -0.52 | 300 | -57 | | | | | |
| B-6 B-6N E | 0.36 | 300 | 30 | 39 | 49 | 037 | 30 | 070 |
| | 0.27 | 300 | | | | | | |
| B-7 B-7N W | -0.21 | 300 | 35 | -23 | 42 | 123 | 61 | 145 |
| | -0.32 | 300 | | | | | | |

TABLE 3 (Cont.) - HORIZONTAL GRADIENT DATA

| STATIONS BASE SUB | CORR. Δg MGALS | DISTANCE FEET | GRADIENT COMPONENTS | | | | THG | | RESIDUAL | |
|-------------------------|--------------------------------|--------------------------|---------------------------------|-----------------|-----|-----|-----|-----|----------|--|
| | | | ECTVOS UNITS U _{xz} | U _{yz} | MAG | AZ | MAG | AZ | | |
| B-8 B-8N W | 0.12 -0.32 | 300 300 | -35 | 13 | 37 | 291 | 38 | 248 | | |
| S-1 S-1N S E W | 0.13 -0.15 -0.26 0.40 | 300 300 300 300 | -28 -44 | 14 16 | 39 | 293 | 38 | 251 | | |
| S-2 S-2N W | 0.05 0.44 | 300 300 | -48 | 6 | 49 | 277 | 53 | 245 | | |
| S-3 S-3N E | 0.19 0.01 | 300 300 | 1 | 21 | 21 | 003 | 7 | 164 | | |
| S-4 S-4N E | 0.06 0.03 | 300 300 | 3 | 7 | 7 | 027 | 21 | 172 | | |
| S-5 S-5N E | 0.07 0.05 | 300 300 | 6 | 8 | 10 | 036 | 22 | 167 | | |
| S-6 S-6N E | 0.21 -0.07 | 300 300 | -8 | 23 | 24 | 341 | 10 | 246 | | |

TABLE 3 (Cont.) - HORIZONTAL GRADIENT DATA

| STATIONS BASE SUB | CORR. Δg MGALS | DISTANCE FEET | GRADIENT COMPONENTS EOTVOS UNITS | | THG MAG | AZ | RESIDUAL | |
|----------------------|---------------------------|------------------|-------------------------------------|----------|------------|-----|----------|-----|
| | | | U_{xz} | U_{yz} | | | MAG | AZ |
| S-7 S-7N E | -0.01 -0.23 | 300 300 | -25 | -1 | 25 | 267 | 40 | 221 |
| S-8 S-8N E | 0.51 -0.36 | 300 300 | -39 | 56 | 68 | 325 | 48 | 304 |
| S-10 S-10S W | -0.25 0.15 | 300 300 | -16 | 27 | 32 | 329 | 17 | 273 |
| S-11 S-11N W | 0.28 0.01 | 300 280 | -1 | 31 | 31 | 358 | 2 | 333 |
| S-12 S-12N W | 0.35 -0.14 | 300 300 | 15 | 38 | 41 | 022 | 19 | 051 |
| S-13 S-13N E | 0.44 0.12 | 300 300 | 13 | 48 | 50 | 015 | 24 | 033 |
| S-14 S-14S E | -0.40 -0.07 | 300 300 | -8 | 44 | 44 | 350 | 17 | 335 |

TABLE 3 (Cont.) - HORIZONTAL GRADIENT DATA

| STATIONS | SUB | CORR. Δg MGALS | DISTANCE FEET | GRADIENT COMPONENTS | | | THG MAG | AZ. | RESIDUAL MAG | AZ |
|----------|------------|-------------------|------------------|---------------------------------|-----------------|----|------------|-----|-----------------|----|
| | | | | ECTVOS UNITS U _{xz} | U _{yz} | | | | | |
| S-15 | S-15N E | 0.16 0.01 | 300 300 | 1 | 18 | 18 | 004 | 11 | 170 | |
| S-16 | S-16N W | 0.26 -0.11 | 300 300 | 12 | 28 | 31 | 023 | 13 | 085 | |
| S-17 | S-17S E | -0.37 -0.20 | 300 300 | -22 | 41 | 48 | 333 | 25 | 301 | |

TABLE 4 - AVERAGE HORIZONTAL GRADIENTS OVER SILIC VENT

| TAKEN AT CENTER OF THE BOX FORMED BY | | TOTAL HORIZ. GRAD. | | RESIDUAL HORIZ. GRAD. | |
|---|------------------|--------------------|-------------|-----------------------|-------------|
| | | MAG E.U. | AZ DEG T | MAG E.U. | AZ DEG T |
| 25N 20N | 25N 3E 20N 3E | 22 | 036 | 21 | 128 |
| 20N 15N | 20N 3E 15N 3E | 29 | 070 | 32 | 125 |
| 15N 10N | 15N 3E 10N 3E | 40 | 032 | 23 | 072 |
| 10N 5N | 10N 3E 5N 3E | 53 | 012 | 27 | 024 |
| 5N 0 | 5N 3E 3E | 54 | 010 | 27 | 020 |
| 0 5S | 3E 5S 3E | 24 | 308 | 24 | 234 |
| 5S 10S | 5S 3E 10S 3E | 13 | 292 | 28 | 207 |
| 10S 15S | 10S 3E 15S 3E | 11 | 109 | 33 | 162 |
| 15S 20S | 15S 3E 20S 3E | 33 | 351 | 6 | 315 |

TABLE 4 (Cont.) - AVERAGE HORIZONTAL GRADIENTS OVER SILIC VENT

| TAKEN AT CENTER OF THE BOX FORMED BY | | TOTAL HORIZ. GRAD. | | RESIDUAL HORIZ. GRAD. | |
|---|--------|--------------------|-------------|-----------------------|-------------|
| | | MAG E.U. | AZ DEG T | MAG E.U. | AZ DEG T |
| 20S | 20S 3E | 5 | 246 | 30 | 188 |
| 25S | 25S 3E | | | | |
| 5W 3N | 3N | 33 | 010 | 8 | 050 |
| 5W | 0 | | | | |
| 3N | 5E 3N | 57 | 023 | 34 | 040 |
| 0 | 5E | | | | |
| 5E 3N | 10E 3N | 50 | 023 | 28 | 046 |
| 5E | 10E | | | | |
| 10E 3N | 15E 3N | 35 | 013 | 11 | 049 |
| 10E | 15E | | | | |
| 15E 3N | 20E 3N | 37 | 345 | 13 | 311 |
| 15E | 20E | | | | |
| 20E 3N | 25E 3N | 39 | 336 | 18 | 297 |
| 20E | 25E | | | | |

TABLE NO. 5

ROCK SAMPLE DENSITIES

| SAMPLE NO. | ROCK TYPE | DENSITY, GMS/CC |
|------------|-----------|-----------------|
| 1 | Rhyolite | 2.25 |
| 2 | Rhyolite | 2.24 |
| 3 | Rhyolite | 2.22 |
| 4 | Rhyolite | 2.24 |
| 5 | Basalt | 2.75 |
| 6 | Basalt | 2.69 |
| 7 | Basalt | 2.64 |
| 8 | Basalt | 2.71 |

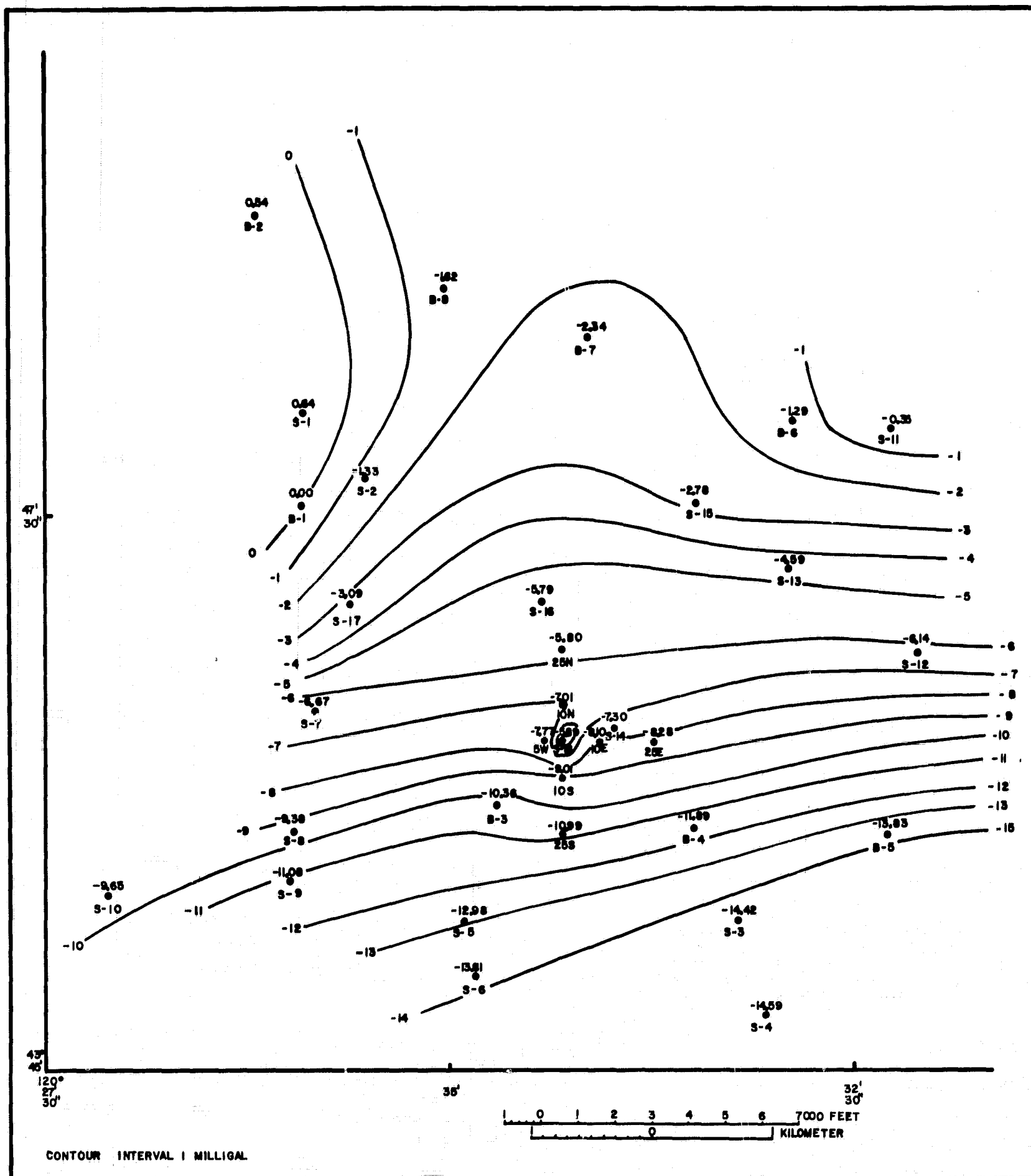


Figure 7. Free-Air gravity anomaly map.

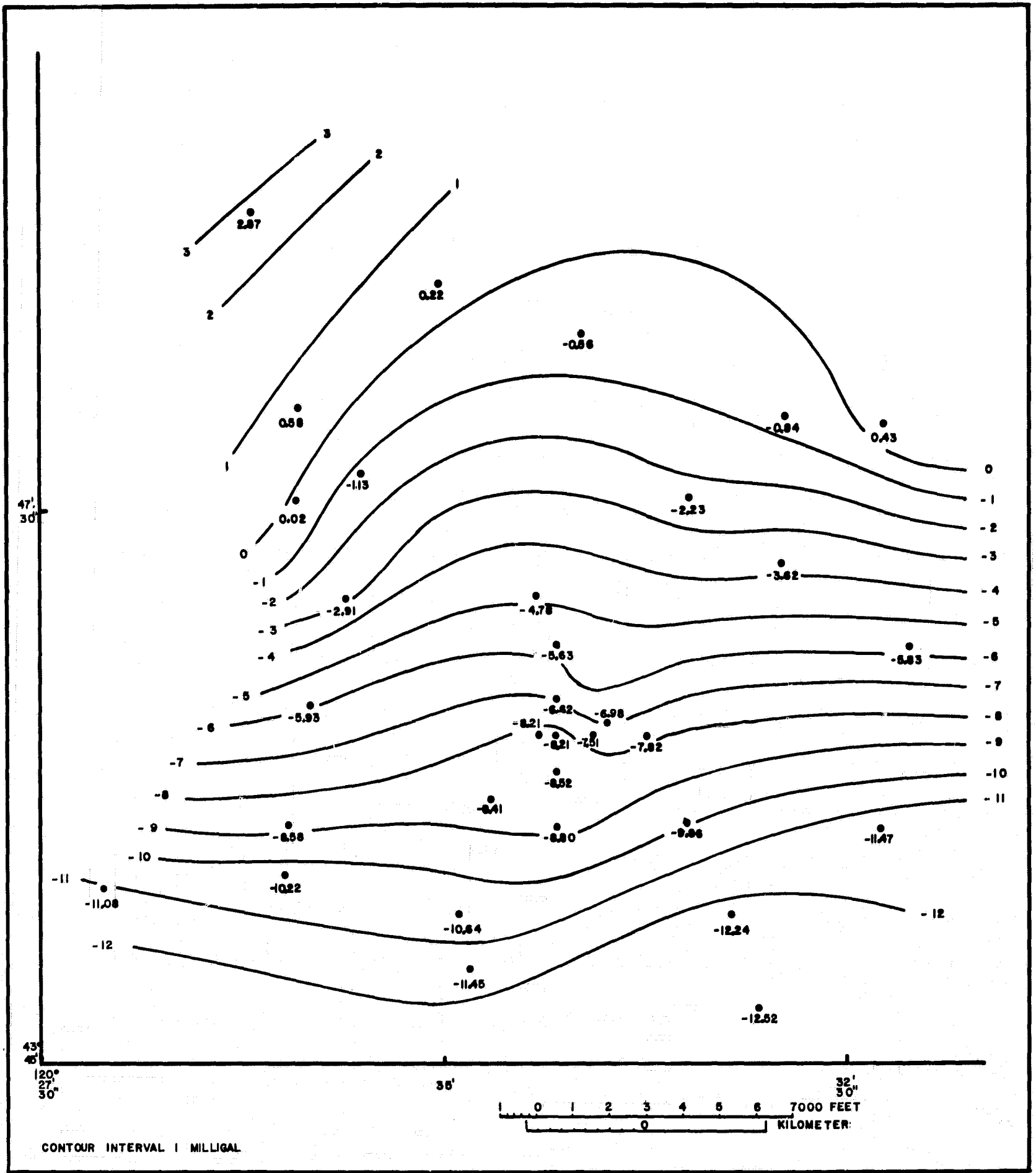


Figure 8. Bouguer gravity anomaly map

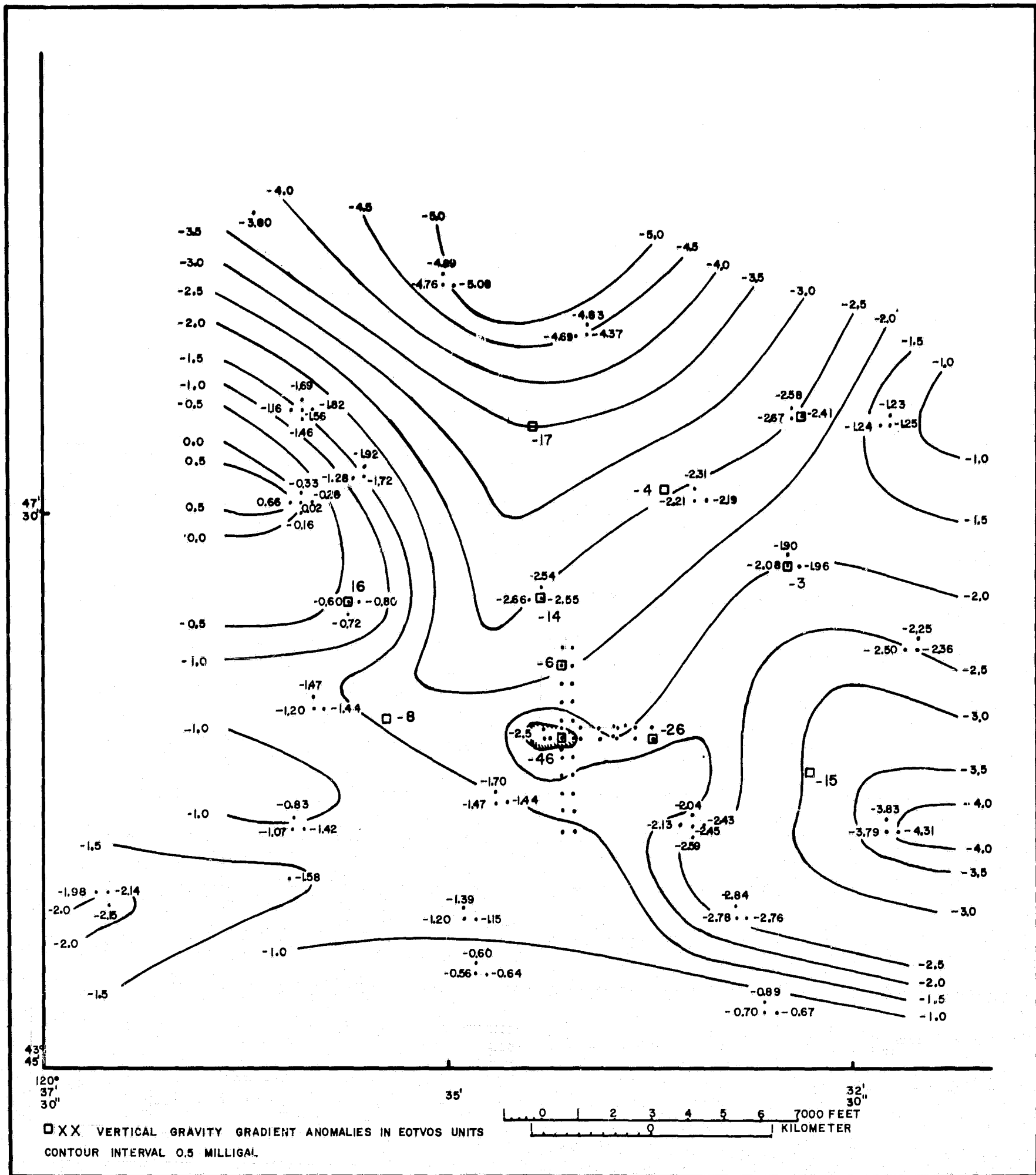


Figure 9. Residual anomaly map.

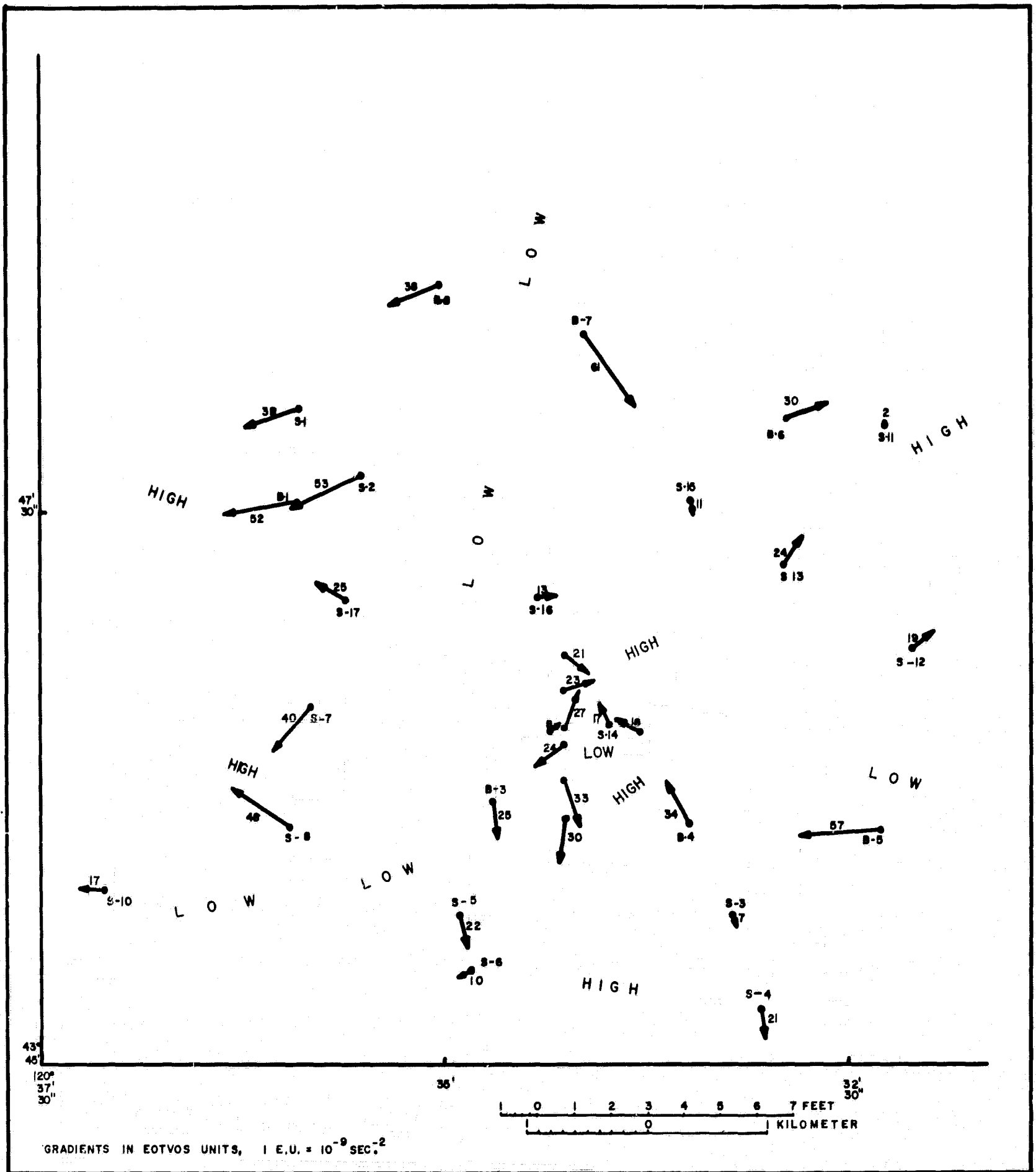


Figure 10. Residual horizontal gradient map.

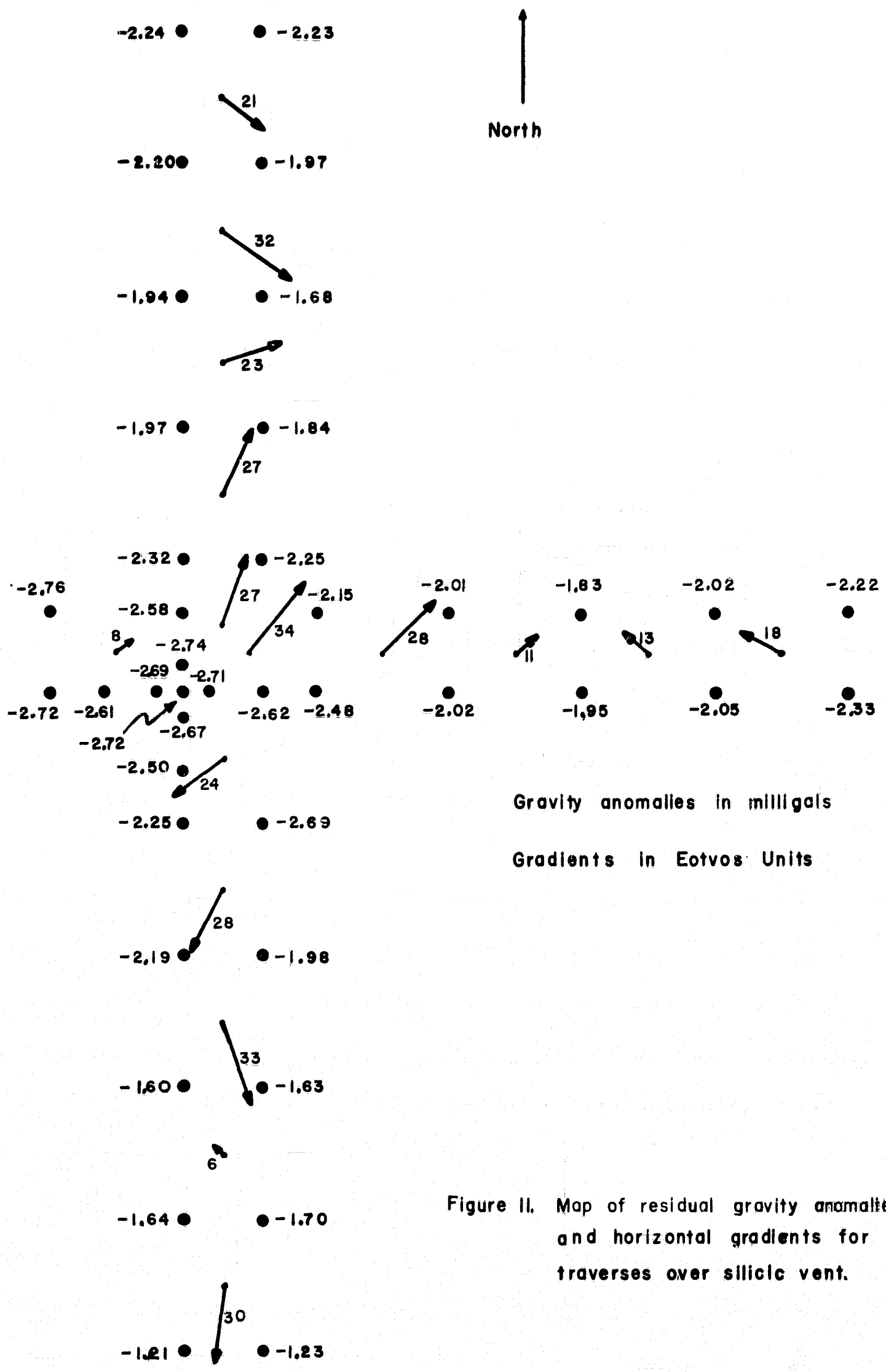


Figure II. Map of residual gravity anomalies and horizontal gradients for traverses over silicic vent.

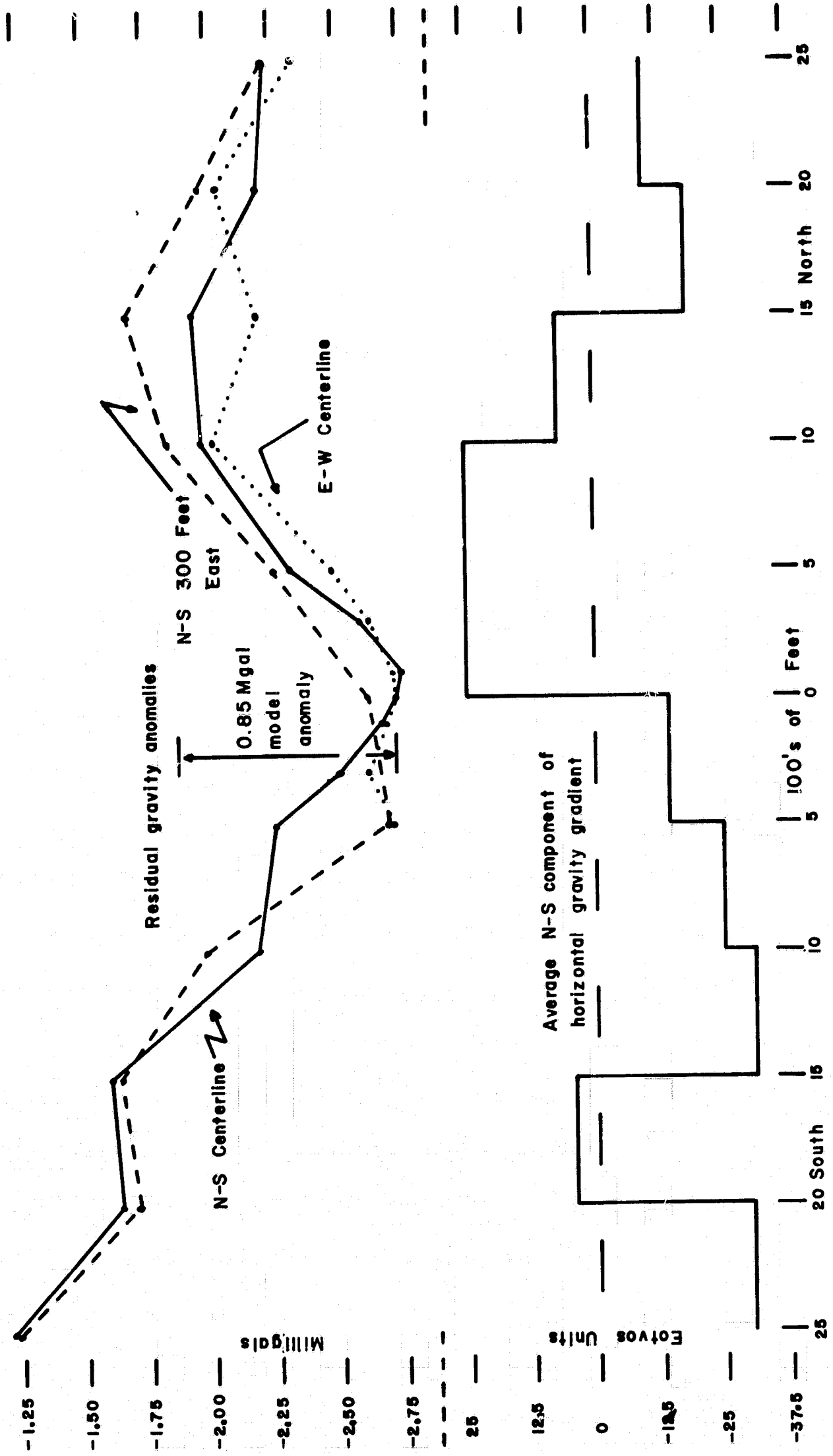


Figure 12. Residual gravity anomaly and horizontal gradient profiles over silicic vent.

VII. INTERPRETATION

The survey area proved to be a complex structure of down-faulted blocks, fractures and faults, lava flows of different densities and a silicic vent.

The Bouguer anomaly map of Oregon (Berg and Thiruvathukal, 1967) with a 10 mgal contour interval shows no anomalies in the survey area other than a bulge in the -140 mgal contour but does indicate the north-trending gradient which is so pronounced in Figure 8. The present survey shows that 2 to 5 mgal anomalies exist in and around the survey area as seen in the residual anomaly map of Figure 9. This anomaly map shows that neither is the fault across the southern part of the area discernable nor is a high or low anomaly totally enclosed within the survey area. However, the map does show an interesting anomaly pattern and feature over the silicic dome which are probably both related. The anomaly map indicates a possible star-like fracture pattern with the silicic vent at its center and alternate sections of down-faulted blocks (gravity lows) or less dense phases of basalt flows radiating from the central vent. This area is, therefore, an example of an obvious zone of weakness in the upper crust and a fracture pattern associated with the occurrence of an upwelling of magma to the surface.

The gravity anomaly pattern gives evidence that rhyolite magma flowed upwards from the east along a fracture (Figures 9 and 11) and extruded on the surface at the junction of the fracture pattern. This was probably the last activity of a great lava flow and the rhyolite (an acid phase) flowed slowly and cooled rapidly to form a cone or dome (which is substantiated by its shape and the fine grained massive rock samples). This might be a typical small volcano cone with a central depression but this is not visible because the entire cone and surrounding plain is covered

by a layer of volcanic ash several feet thick. The gravity anomaly over the dome (Figure 12) is only about -0.85 milligals which indicates there is not much depth to the feature other than the topographic expression. In fact, it is a very small geologic feature. The gravity profiles also indicate a reasonable symmetry of the cone and therefore it can be represented by a series of vertical cylinders or discs. A model of the vent cone which satisfies the physical dimensions of the hill and gives the proper peak gravity anomaly is shown in Figure 13. The rhyolite dome is represented by a set of discs and a thin vertical cylinder for the vent tube. The density contrast between the rhyolite dome and the surrounding basalt is 0.50 gms/cc. The actual gravity anomaly profile over the dome is shown in Figure 12 together with the calculated peak anomaly of the model structure. There is excellent agreement between the actual and calculated peak values and it appears obvious that the vent cone is similar to the shape of the model. This small but very interesting geologic and volcanic feature could be similar to the small dome-like features on the moon which occur in the Maurius Hills region (Hess et al, 1969).

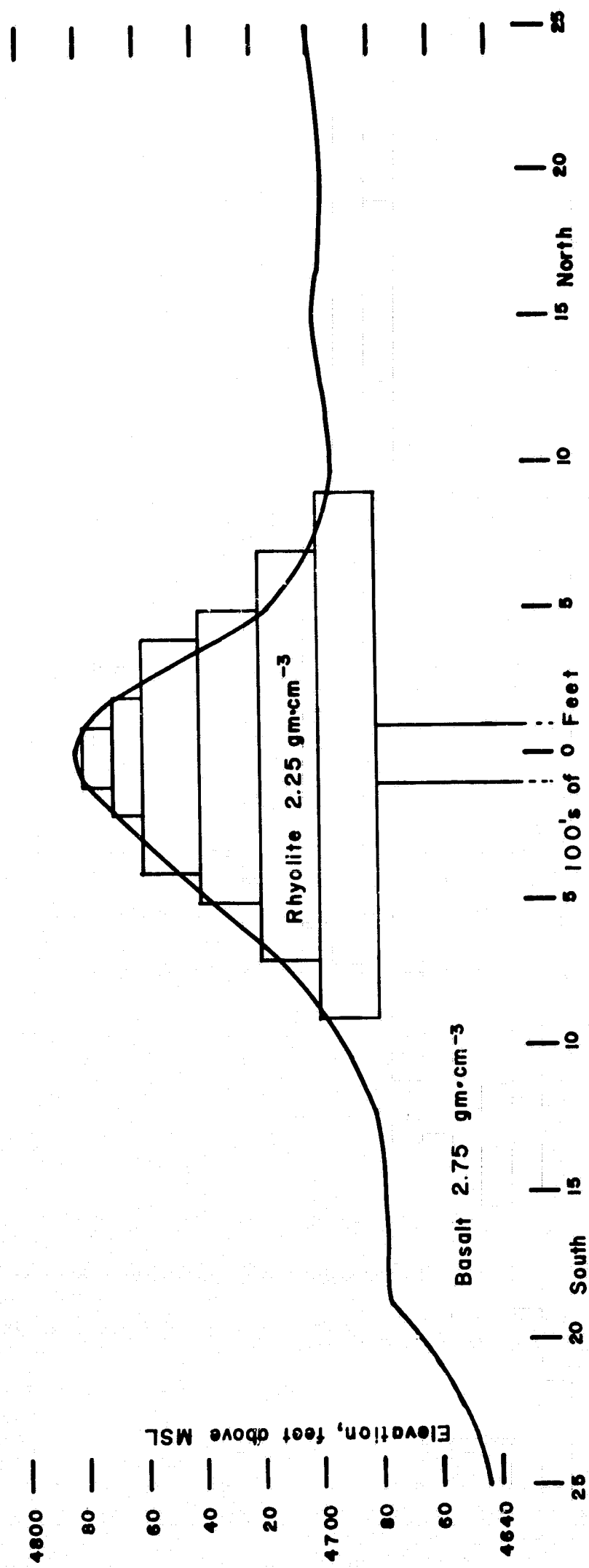


Figure 13. Interpretive model of silicic vent.

VIII. DISCUSSION

The gravity anomalies of Figure 9 are defined essentially from gravity stations at about 1 km interval and are thus related to geologic structures 2 km or more in extent. On the other hand, the horizontal gradient anomalies in Figure 11 are primarily caused by smaller nearby anomalous masses which may be a few thousand feet or less in extent. The presence of these smaller structures is also indicated by the rapidly changing gravity values at 300 ft. intervals on Figure 9. These small features are not defined in Figure 9 by reason of a lack of stations. Thus the gravity anomaly map (Figure 9) reflects larger structural features while the horizontal gradient map tends to reflect smaller nearby structures.

The data gathering, reduction and plotting for the horizontal gradient technique proved to be relatively easy compared to the equivalent conventional gravity method. The hardest part of a conventional gravity survey is the precise levelling of each station which, in this case, was required chiefly for only the traverses over the silicic vent hill. If levelling had been required for all the gravity stations in the survey area, the acquisition of the gravity data would have been prohibitively difficult, time consuming and expensive. The precise elevation of each main station is not required for the gradient method. The levelling of the auxiliary gravity gradient stations relative to the main station is relatively easy and involves very little extra work by the survey party. If a vertical gravity gradiometer were to be used, no levelling of the stations would be required but any nearby local topography should be mapped for terrain corrections. It thus appears that vertical gravity gradient surveying would be the simplest and easiest method. Where a limited number of observation points is available, (such as on a single traverse), the horizontal gradients are more informative than the gravity

values because the horizontal gradient vectors also indicate the direction to a mass of higher density. The availability of horizontal gradient data helps in the contouring of a gravity anomaly map and conversely the gravity anomalies help in the interpretation of the horizontal gradient map. Since the vertical gravity gradients shown on Figure 9 have been calculated from the pattern of larger anomalies they do not include the effects of nearby smaller masses and are, therefore, "average" gradients. Direct observations made at these points with a vertical gradiometer would probably reflect the effects of small, nearby structures. For comparison purposes, several direct vertical gradient measurements around each calculation point will likely be required to give a mean vertical gradient equivalent to the calculated values. In spite of this, the calculated vertical gradients will serve as a reference for the comparison of future measurements made with a vertical gravity gradiometer.

IX. CONCLUSIONS

1. This field test survey permitted a first-hand comparison of the gravity gradient surveying technique with the conventional gravity method and illustrated the utility and advantages of the gradient method. Generally speaking, the horizontal gradient method was easier and more efficient because it involved less work in levelling and less data processing in spite of the greater number of gravity measurements required. If no elevations are available and a large area (such as 5 km x 5 km) is to be surveyed, there is no question that the horizontal gradient method is easier. Trends or areas of high and low density masses can be inferred directly from a map of horizontal gradients but direct contouring and interpretation of high and low density features is difficult since no suitable methods of direct interpretation have been developed as yet. The horizontal gradient technique proved to be useful for single profiles or where a limited number of observation points is available because it has the advantage that gradient vectors indicate areas of high and low density (gravity values generally do not). The gradient technique also proved to be effective for the detection of small nearby features.

By the conventional gravity method, a gravity anomaly map does not reflect small anomalies for this type of survey but is good for outlining larger features, since gravity is sensitive to larger, more distant features. The detection capability by the gravity method depends a great deal on the station spacing but for very small features gravity measurements become less effective. The gravity method has the distinct advantage that gravity values can be contoured directly and readily to define areas of high and low density. Also, interpretation methods for gravity anomalies have been well developed and are standard practice.

Potentially, vertical gravity gradient surveying offers most of the advantages of both the horizontal gradient technique and the conventional gravity method. No precise levelling is required and more stations could be rapidly observed to map anomalies in greater detail. Less field work, data reduction, processing and plotting is necessary as in the case of horizontal gradients. The vertical gradient values can be plotted and contoured directly in magnitude as in the gravity anomaly method. The vertical gradient measurements would be most effective for detecting small nearby anomalies but also, with appropriate field measurement procedures, average or regional vertical gradients could be determined.

Vertical gravity gradient values calculated from the gravity anomaly map of the survey area will provide reference and control values for future tests with a vertical gravity gradiometer.

2. This field test survey also gave valuable first-hand experience and information concerning the anomalies over features similar to those expected on the moon in a 5 km radius area. Within the 5 km x 5 km survey area, anomalies of only 2 to 5 mgal were observed as well as a small 0.85 mgal anomaly over a silic vent dome. This dome proved to be an interesting feature appropriate for gravity gradient studies. However, the topographic expression of the feature was somewhat undesirable for this test. The known fault across the southern portion of the area proved to have no significant gravity anomaly. This indicates that the fault does not extend to any depth and is probably only the surface topographic scarp itself. These results indicate that gravity anomalies of only a few milligals may exist over features within a 5 km radius area on the moon and less than 1 mgal anomalies may be associated with smaller volcanic features such as the domes in the Maurius Hills region. It, therefore, appears that accurate gravity measurements, levelling and positioning are required to define such

anomalies for lunar exploration. The gravity gradient method, particularly the vertical gradient if suitable instrumentation can be developed, appears to be more effective for exploring the smaller features to be found in a 5 km radius area.

3. This survey also provided supplemental gravity data for the gravity map of Oregon. This data will also aid the seismic study of the area and subsequent geologic structure analysis. In particular, the survey outlined a fracture zone and pattern associated with a volcanic vent and lava flow.

X. RECOMMENDATIONS

1. The gravity survey of this area should be extended at least another 5 km in all directions to completely enclose the gravity highs and lows and complete the anomaly pattern. A reconnaissance survey of a much larger area would be desirable to identify a more isolated and usable anomaly associated with a larger specific subsurface geologic feature.

2. Preliminary vertical gravity gradient measurements with a vertical gradiometer should be made at the points in the survey area where vertical gradients have been calculated. A detailed vertical gradient traverse over the rhyolite dome could also be performed to advantage. It is singularly important that vertical gradient measurements be made to provide a comparison of this method with that of the horizontal gradient and gravity methods and to verify the utility and advantages of the method. Initially, preliminary measurements could be made with the available laboratory gradiometer at the existing vertical gradient points. After the development and fabrication of a prototype portable field gradiometer, a detailed vertical gradient survey could be performed over the entire area as well as detailed traverses across the rhyolite dome.

3. Just as survey techniques were developed over the years for successful gravity surveying, so new techniques will have to be developed for gradient surveying. Future test programs should, therefore, include an active and concentrated work effort for the development of gradient surveying techniques.

4. Present gradient survey results have indicated a lack of interpretation techniques. It is recommended, therefore, that a follow-on program should include the development of direct interpretation techniques for gradient surveys.

ACKNOWLEDGMENTS

We would like to thank the following for their cooperation and assistance: Mr. Henry McCormick, Supervisor, Forest Service, Bend, Oregon who gave us valuable advice for operating in the area; Mr. Dwight Conley, Bureau of Land Management, Department of the Interior, Prineville, Oregon who gave us permission to work on the BLM lands as well as much helpful information about the survey area; Mr. Keith Westhusing, Lockheed Electronics Company, Houston, Texas who kindly performed an early reconnaissance of the survey area and investigated available local services; Dr. H. Richard Blank, University of Oregon, Eugene, Oregon who provided unpublished data on the gravity meter calibration line and several gravity reports and maps for use during the survey. The contributions of William B. Chapman, Technical Monitor, are gratefully acknowledged.

REFERENCES

- Berg, J. W. and J. V. Thiruvathukal, Gravity maps of Oregon (onshore and offshore), State of Oregon Department of Geology and Mineral Industries, No. 4 of Geologic Map Series, 1967.
- Blank, H. R. and D. F. Barnes, Crater Lake calibration loop, Unpublished manuscript, University of Oregon, Eugene and U.S. Geologic Survey, Menlo Park, California, 1969.
- Brothers Quadrangle, Oregon, 7.5 minute series (topographic) N4345-W12030/7.5 U.S. Geologic Survey, Washington, D.C. (1967).
- Dobrin, M. G., Introduction to geophysical prospecting, McGraw-Hill, New York, 1960.
- Grant, F. S. and G. F. West, Interpretation theory in applied geophysics, McGraw-Hill, 1965.
- Hess, W., R. Kovach, P. W. Gast and G. Simmons, The exploration of the Moon, Scientific American Vol. 221(4) 54-72, Oct. 1969.
- Muller, P. M. and W. L. Sjogren, Mascons: lunar mass concentrations, Science, 161, 680-684, 1968.
- Rinehart, W., R. G. Bowen and E. F. Chiburis, Airport gravity base station network in Oregon, The Ore Bin (State of Oregon Dept. of Geology and Mineral Industries), 26(2), 37-42, 53-56, 1964.
- Thompson, L. G. D., M. H. Houston and D. A. Rankin, Gravity gradient preliminary investigations. General Oceanology Report No. 9, NASA Contract NAS 9-9200, 1969.

REFERENCES (Cont.)

Thyssen-Bornemiza, S., Double track profiling with the the gravity meter, Geophysics, XXX(6), 1135-1137, 1965.

Thyssen-Bornemiza and W. F. Stackler, The average horizontal gravity gradient, Geophysics, XXVII(5), 714-715, 1962a.

Thyssen-Bornemiza and W. F. Stackler, A possible application to geophysical exploration of the average horizontal gravity gradient using the gravity meter, A.P.E.A. Journal, 1962b.

Walker, G. W., N. V. Peterson and R. C. Greene, Reconnaissance geologic map of the east half of the crescent quadrangle Lake, Deschutes, and Crook counties, Oregon, U.S. Geologic Survey, Washington, D.C. 1967.

PART II

LUNAR MASCON GRAVITY GRADIENTS

I. INTRODUCTION

This report covers the results of a preliminary investigation of gravity gradients associated with lunar mass concentrations (Mascons) performed under Exhibit "B" of the Statement of Work of Contract NAS 9-9200.

The purpose of this work was to give a preliminary assessment of the usefulness of gravity gradients for aiding in the exploration and interpretation of mass anomalies on the moon. In addition, the magnitudes of the gradients over known lunar gravity anomalies are of particular interest for future lunar orbital and surface experiments. In performing this study, gravity gradient profiles over two Mascons centered on Mare Imbrium and Mare Serenitatis were calculated from their gravity anomalies. The gradient profiles or signatures were then used to illustrate their application in the interpretation of the Mascons.

II. GRAVITY GRADIENT TECHNIQUES

In theory, the "gradient of gravity" is the second derivative of the gravitational potential and is a nine-component tensor function of position. In practice, the gravity gradient components of particular interest that can be measured as scalar quantities are: (a) the vertical gravity gradient (U_{zz})* which is the vertical rate of change of the vertical component of gravity, and (b) the horizontal gravity gradients in the X and Y directions (U_{zx} , U_{zy}) which are the horizontal rates of change of the vertical component of gravity in the X and Y directions.

Varying density distributions within the earth's crust cause gravity gradient anomalies as well as gravity anomalies, hence geologic structures may be detected and identified by their gravity gradient signatures.

Table 1 presents equations for the gravity anomaly, the vertical gravity gradient anomaly and the horizontal gravity gradient anomaly for three simple geologic models of a sphere, a two-dimensional horizontal cylinder, and a two-dimensional fault. A computer program to calculate the gravity anomalies and gravity gradients over two-dimensional structures of arbitrary shape by the method of Talwani, Worzel, and Landisman (1959) is listed in Appendix A. Figure 1 shows a plot of the gravity anomaly and vertical and horizontal gradients caused by a sphere. The vertical gradient peaks over the center of the sphere, decreases more rapidly with increasing distance from the origin than the gravity anomaly,

* Subscripts denote differentiation:

U = gravitational potential

U_z = $\frac{\partial U}{\partial Z}$ = vertical component of gravity; Z is the vertically down direction

U_{zz} = $\frac{\partial U_z}{\partial Z} = \frac{\partial^2 U}{\partial Z^2}$ = vertical gravity gradient.

TABLE 1
EQUATIONS FOR GRAVITY AND GRAVITY GRADIENT ANOMALIES FOR SIMPLE MODELS

| MODEL | GRAVITY | | GRADIENTS | | |
|---------------------|-----------------------|---------------------------------|----------------------------|---|------------------------------------|
| | Normalization Factor | Anomaly | Normalization Factor | Vertical Anomaly | Horizontal Anomaly |
| Sphere | $\frac{U_z}{-GM/Z^2}$ | $\frac{1}{(1 + X^2/Z^2)^{3/2}}$ | $\frac{U_z(z,x)}{2GM/Z^3}$ | $\frac{1 - X^2/Z^2}{(1 + X^2/Z^2)^{5/2}}$ | $\frac{3X/Z}{(1 + X^2/Z^2)^{5/2}}$ |
| Horizontal Cylinder | $\frac{U_z}{-GM/Z}$ | $\frac{1}{(1 + X^2/Z^2)}$ | $\frac{U_z(z,x)}{GM/Z^3}$ | $\frac{1 - X^2/Z^2}{(1 + X^2/Z^2)^2}$ | $\frac{2X/Z}{(1 + X^2/Z^2)^2}$ |
| Fault | $\frac{U_z}{-2GM}$ | $\frac{\pi}{2} - \tan^{-1} X/Z$ | $\frac{U_z(z,x)}{2GM/Z}$ | $\frac{-X/Z}{1 + X^2/Z^2}$ | $\frac{1}{1 + X^2/Z^2}$ |

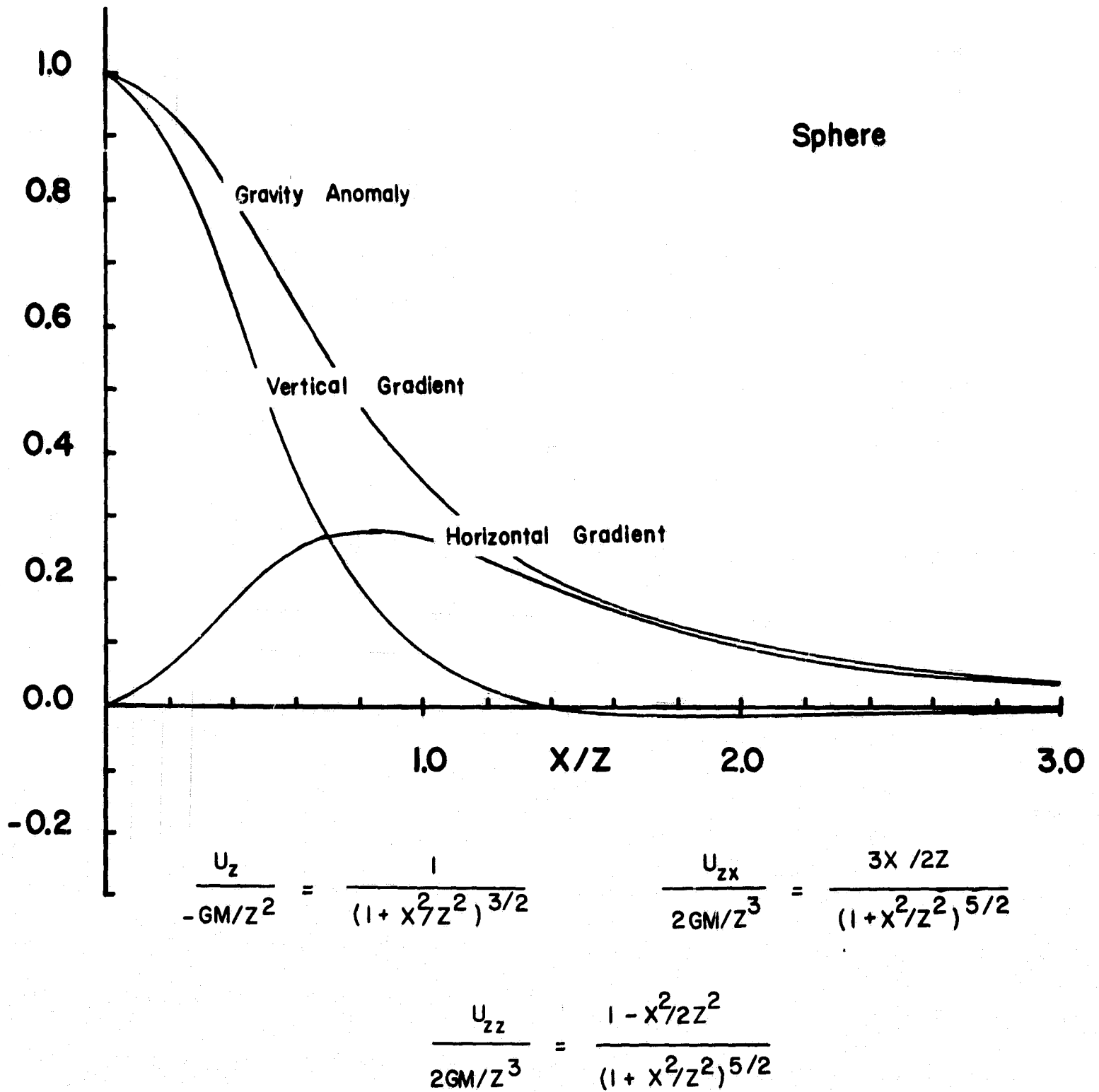


FIGURE 1 - Normalized profiles of gravity anomaly, vertical gradient and horizontal gradient over a sphere centered beneath the origin.

and eventually decreases to a negative value. The horizontal gradient changes sign at the origin and reaches a local maximum that is a fraction (about 0.26) of the vertical gradient peak value. Figure 2 presents the gravity and gradient signatures for a semi-infinite horizontal cylinder. The vertical gradient peaks over the center of the cylinder, decreases more rapidly with increasing distance from the origin than the gravity anomaly, and crosses to a negative value when the lateral distance from the center of the cylinder equals the depth to the center of the cylinder. The horizontal gradient is antisymmetric about the origin and the local maximum is a fraction (about 0.65) of the vertical gradient peak value. Figure 3 presents the signatures for a fault. The normalized gravity anomaly is antisymmetric about the line at $y = \pi/2$ and is asymptotic to π and zero. The gradient signatures for the fault can be easily distinguished from the signatures of the sphere or cylinder. The vertical gradient is antisymmetric about the origin and peaks not above the fault-line, but reaches a local maximum (-0.5) at a lateral distance equal to the depth to the center of mass. (For convenience the negative value of the vertical gradient has been plotted in Figure 3.) The horizontal gradient is symmetric about the fault-line and decreases asymptotically with lateral distance from the origin. The two dimensional fault is one of the few cases in which the peak value of the horizontal gradient exceeds the peak value of the vertical gradient.

Table 2 compares several characteristics of the gradient signatures for the three models. For the sphere and the horizontal cylinder the vertical gradient peaks over the structure's centerline but has a different shape for each structure. The horizontal gradient is antisymmetric and reaches a maximum on the flanks of the disturbing body at a scaled distance which is characteristic of the model. The signatures for the fault are

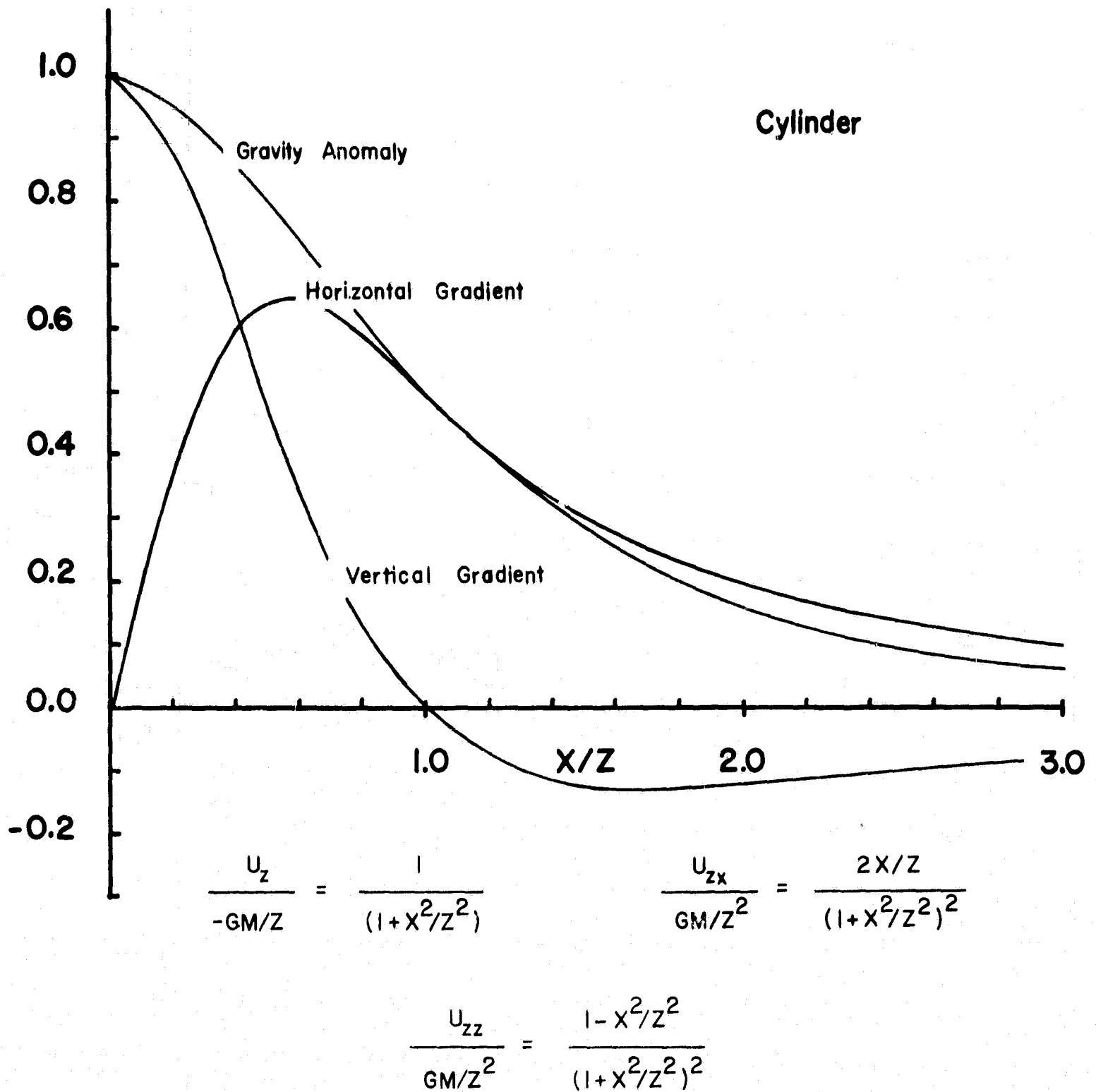
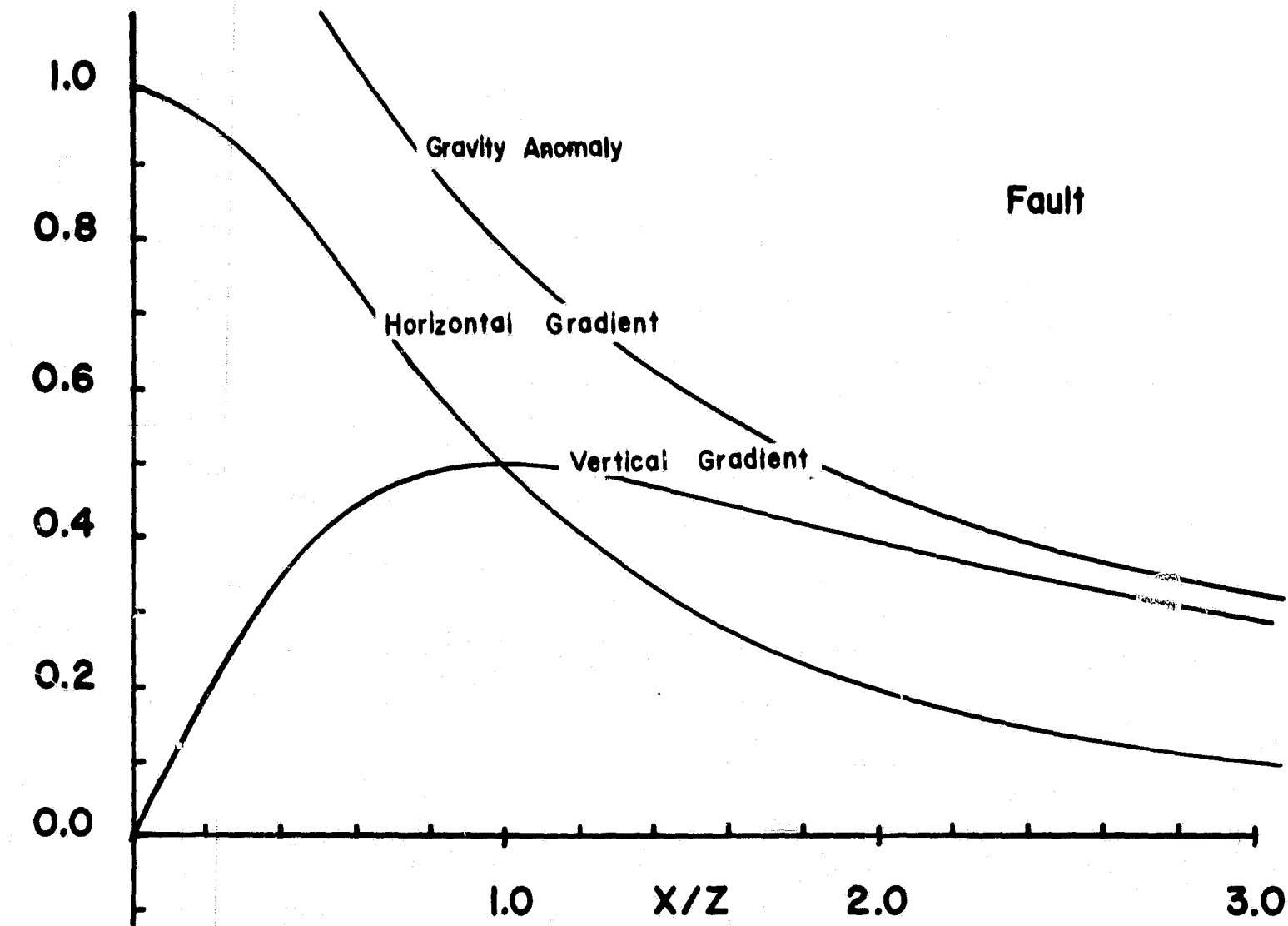


FIGURE 2 - Normalized profiles of gravity anomaly, vertical gradient and horizontal gradient over a semi-infinite horizontal cylinder centered beneath the origin.



$$\frac{U_z}{2GM} = \frac{\pi}{2} - \tan^{-1} \frac{X}{Z} \qquad \frac{U_{zx}}{2GM/Z} = \frac{1}{(1+X^2/Z^2)}$$

$$\frac{U_{zz}}{2GM/Z} = \frac{-X/Z}{(1+X^2/Z^2)}$$

FIGURE 3 - Normalized profiles of gravity anomaly, vertical gradient and horizontal gradient over a semi-infinite fault. The fault-line is centered beneath the origin.

TABLE 2

COMPARISON OF CHARACTERISTICS OF
GRADIENT SIGNATURES FOR SIMPLE MODELS

| | Sphere | Horizontal Cylinder | Fault |
|---|---------------|---------------------|-----------------|
| | $\pm X/Z$ | $\pm X/Z$ | $\pm X/Z$ |
| $U_{zz} = \text{Maximum}$ | 0 | 0 | ± 1.0 |
| $U_{zz} = 0$ | 1.4, ∞ | 1.0, ∞ | 0, $\pm \infty$ |
| $U_{zx} = \text{Maximum}$ | 0.8 | 0.6 | 0 |
| $U_{zx} = 0$ | 0, ∞ | 0, ∞ | $\pm \infty$ |
| $U_{zz}/U_{zz \text{ max}} = 1/2$ | 0.5 | 0.5 | 0.3 & 4.0 |
| $U_{zx \text{ max}}/U_{zz \text{ max}}$ | ± 0.3 | ± 0.7 | ∓ 2.0 |
| $U_z \text{ max}/U_{zz \text{ max}}$ | $Z/2$ | Z | $2\pi Z$ |

distinctly different. Figures 1, 2 and 3 and Table 2 show that different structures have different signatures of U_z , U_{zz} , and U_{zx} and also, more important, the different structures have different combinations of signatures. Thus, with multiple signatures the type of structure can more readily be identified and classified than with only one signature.

As a further example, Figure 4 presents the gravity and vertical gradient signature over a flat plate. The gravity and vertical gravity gradients have been calculated using a numerical approximation method outlined in Appendix B. The horizontal gradient has not been plotted but can easily be obtained from the gravity anomaly profile. The gravity anomaly profile has a broad peak with relatively steep sides. The vertical gradient profile has a local positive minimum at the center of the disk, a local maximum located in a ring near the edge of disk, and steep sides which fall to a ring of negative gradient values just beyond the edge of the disk. This gradient signature is distinctly different from the signatures of the preceding models.

In summary, it is evident that the gravity gradient technique can be used effectively for the exploration and interpretation of geologic structures. Different features can be identified by their gradient signatures equally as well as by their gravity anomaly signature. Moreover, additional structural detail can be obtained from sampling the gradient (particularly the vertical gradient) as well as sampling the gravity anomaly. Although solutions obtained with the aid of gradients are not mathematically unique (in the same sense that gravity solutions are not unique), they do reduce the number of possible solutions to a lower order.

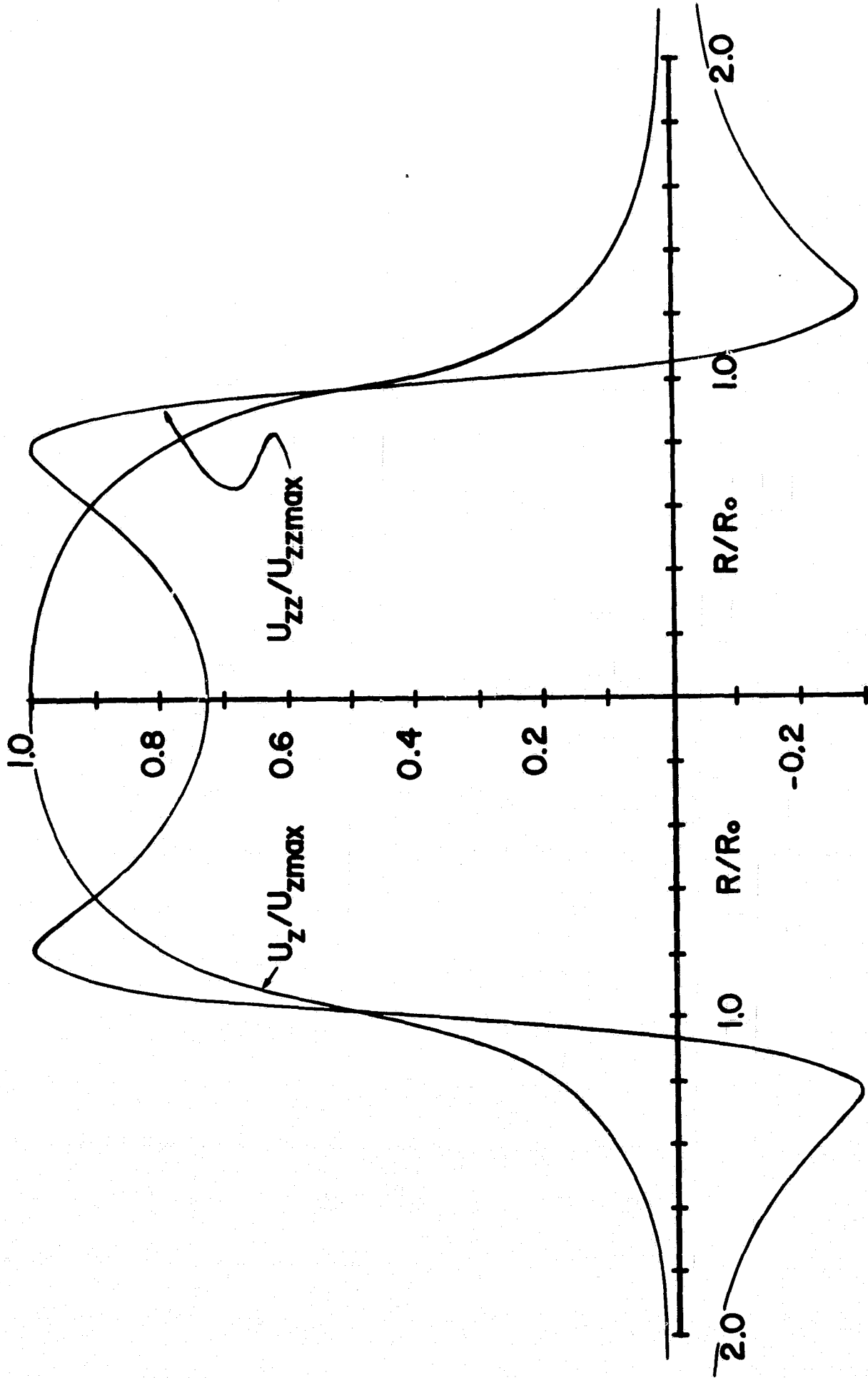


FIGURE 4 - Normalized profiles of vertical gravity anomaly and vertical gradient over a flat plate. The model is 100 km in radius, 15 km thick, buried 20 km, and has a density contrast of 1.0 gms/cm^3 . The peak gravity anomaly is 168.4 mgals and the maximum vertical gradient is 27.2 E.U. 1 Eotvos Unit (E.U.) = $10^{-9} \text{ cm/sec}^2/\text{cm}$.

III. APPLICATION OF GRADIENT TECHNIQUES TO LUNAR MASCONS

A. LUNAR GRAVITY DATA

The first measured gravity anomalies on the moon were determined by Muller and Sjogren (1968) by the technique of doppler tracking of lunar satellite velocity perturbations. Other work to improve the data has been reported* but the basic source of gravity data has not changed. At the time of this investigation, the original data of Muller and Sjogren in the form of a gravity anomaly map was the only accepted reference available.

It must be stressed that the lunar gravity field determined from satellite tracking yields the equivalent of Free-Air anomalies. On the earth the Free-Air anomalies primarily reflect the topography of the land masses because the structural density changes in the crust have smaller effects on the observed gravity than the actual excesses of mass produced by the topographic features. Generally speaking, such anomalies exhibit positive values over the continents and negative values over the oceans. For geophysical exploration on land surfaces, Free-Air anomalies are generally not suitable for most interpretive studies. Bouguer anomalies, which remove the effects of topography, are preferred. On the earth, the Bouguer anomalies are usually the inverse of the Free-Air anomalies and generally exhibit a negative anomaly over the continents (indicating a lower density material within the earth's crust) and a positive anomaly over the oceans (indicating a higher density material). For this study, therefore, a Bouguer anomaly map is considered to be the most appropriate gravity data for the interpretation of the Mascons and for investigating the application of the gradient techniques.

* Kane, 1969; Muller and Sjogren, 1969; Blackshear, 1969; Gottlieb and Laing, 1969; Wong, Buechler, Downs and Prislín, 1969; Lorell, 1969.

A suitable Bouguer anomaly map has already been prepared by O'Keefe (1968) from the original Free-Air anomaly map of Muller and Sjogren. O'Keefe's map was, therefore, used as the basic reference data for this gradient investigation. A reproduction of O'Keefe's map plotted on an equal area projection is shown in Figure 5. The contours of O'Keefe have been extended north of 40°N consistent with the Free-Air anomalies of Muller and Sjogren and with lunar topography.

B. METHOD OF GRADIENT CALCULATION

Horizontal gradients can be approximated from the gravity data by a finite difference method. If a gravity anomaly profile is plotted, the horizontal gradient at any position is the slope of the gravity profile at that position. The vertical gradient requires a more involved approximation procedure.

After examination of several methods* for calculating vertical gradients, the following procedure was selected as being most suitable for the lunar Mascon case. As shown by Grant and West (1965), p. 221, the vertical gradient can be obtained by:

$$\text{Eq. (1)} \quad \lim_{z \rightarrow 0} \frac{\partial U_z}{\partial z} = - \frac{U_{z_0}(0)}{\epsilon} + \int_{\epsilon}^{\infty} \frac{U_z(r)}{r^2} dr ,$$

where ϵ = radius of a small, finite circle surrounding the point of origin in which U_z does not sensibly change from its value at $r = 0$; $U_{z_0}(0)$ = gravity value at origin.

* For example: Baranov, V., 1957; Raspopov, O. M., 1958; Raspopov, O. M., 1959; Chinnery, M. A. 1961.

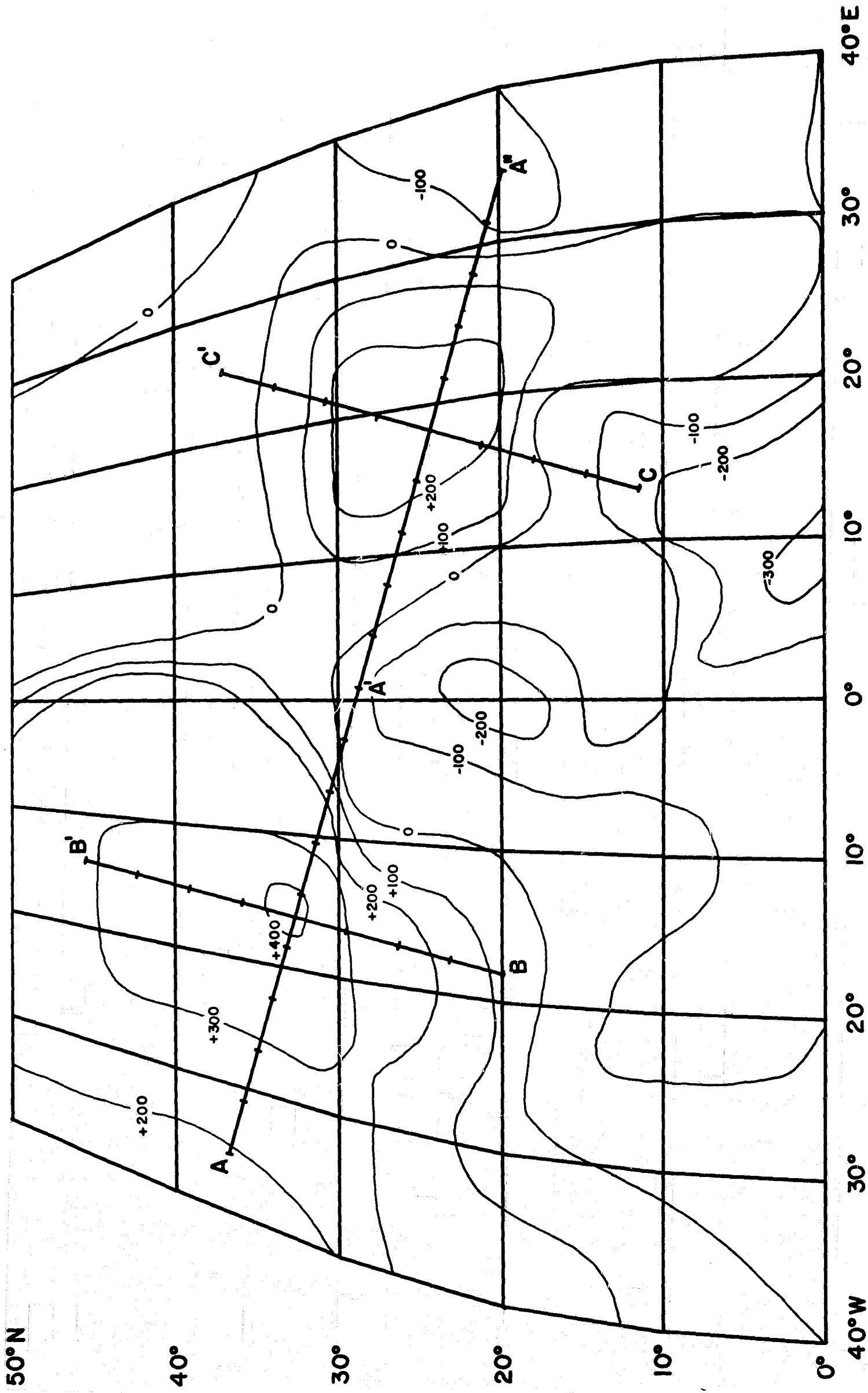


FIGURE 5. Bouguer anomaly map of the moon after O'Keefe (1968). The map is an equal area projection with isogals every 100 milligauss. Profile lines are indicated: A-A' and B-B' cross Mare Imbrium; A'-A'' and C-C' cross Mare Serenitatis. Marks every 100 km indicate calculation positions for vertical and horizontal gradients.

In principle, at least, the integral of Equation 1 in which U_z is not a function but a field of values on a plane surface, can be approximated by using a template or overlay. The template is sectioned into convenient divisions of radius r , and angle, θ , and the average value of U_z within each segment is estimated. The gradient estimator then becomes

$$\text{Eq. (2)} \quad U_{zz} = \frac{U_{z_0}}{r_0} + \sum_{i=1}^N \overline{U_{z_i}} \left[\frac{1}{r_{i-1}} - \frac{1}{r_i} \right]$$

The accuracy of the approximation is limited not only by the ability of the operator to correctly estimate the average anomaly in each segment, but also by the nature of the weighting functions in the integral. The weighting function attaches greatest importance to values near the origin, and with a template, excludes contributions to the gradient beyond a certain distance from the origin. Any uncertainty in the contouring near the origin would lead to uncertainty in the gradient. Similarly, small scale fluctuations in gravity near the origin could dominate larger, possibly more significant trends.

A gradient template to calculate the vertical gradient from O'Keefe's map of lunar Bouguer anomalies (Figure 5) was constructed with ring radii of 10, 30, 50, 90, 130, 210, and 300 km. For these dimensions an uncertainty of ± 10 mgals in the average gravity anomaly within the 10 km ring gives an uncertainty of ± 10 E.U.* in the vertical gravity gradient at the origin. A

* 1 Eotvos Unit (E.U.) = 10^{-9} cm/sec²/cm.

difference of ± 100 mgals between the gravity anomaly at the origin and gravity in a ring 700 km beyond the outer template ring (300 - 1000 km) results in an uncertainty of about ± 2 E.U. for U_{zz} at the origin.

Two tests of the validity of the gravity gradient estimator were carried out. In the first test the gradient was estimated over a sphere which was buried at a depth of 100 km and which gave a peak anomaly of 210 mgals. The estimated vertical gradient was within 10% of the calculated gradient for lateral distances of 0, 40, and 100 km from the center of the sphere. A second test was performed using the gravity anomaly for the flat plate model shown in Figure 4. Again, the estimated gradients were within 10% of the calculated gradients for distances of 0, 80, and 120 km from the center of the disc. The bias of the estimated gradients was not constant.

The method is certainly adequate to at least delineate the character of the vertical gradient profile for each model, but is not adequate to make fine quantitative distinctions between two structures with similar gradient signatures. Accuracy and quality of the gravity data is as much to blame as the crudity of the template method. In the future, better gravity data could be processed more accurately with a finer template. The ideal situation would be to measure the gradients directly; lacking measured gradients, more precise gravity data in greater density is needed to improve the gradient approximation.

IV. RESULTS

Selected profile lines along which gradients have been calculated are shown in Figure 5. Profiles A-A' and B-B' cross Mare Imbrium; A'-A'' and C-C' cross Mare Serenitatis. Figures 6 through 9 illustrate the gravity anomaly profiles over the respective Mascons. The gravity anomaly profiles were constructed using the 100 milligal contours plus additional contours interpolated every 50 milligals.

Gradients were calculated every 100 km along the profile lines. Horizontal gradients were calculated by computing the gravity anomaly change in 100 km centered on the 100 km marks. The horizontal gradients are presented in Figures 10 through 13. The vertical gradients were calculated using the template method discussed above. Figures 14 through 17 present the profiles of the vertical gravity gradients.

The order of magnitude of the gradients is an important result. The value of the horizontal gradients ranged from +10 to -20 E.U. with about 20% of the estimated horizontal gradients exceeding an absolute value of 10 E.U. As expected the vertical gradients were generally greater in magnitude than the horizontal gradients. The vertical gradients ranged from +38 E.U. to -20 E.U. with about 20% of the estimated vertical gradients exceeding an absolute value of 20 E.U. In general, the vertical gradient profiles were not symmetric with respect to the peak value. The maximum range between minimum and maximum values of the gradient in any single profile was about 50 E.U. for the vertical gradient and about 35 E.U. for the horizontal gradient.

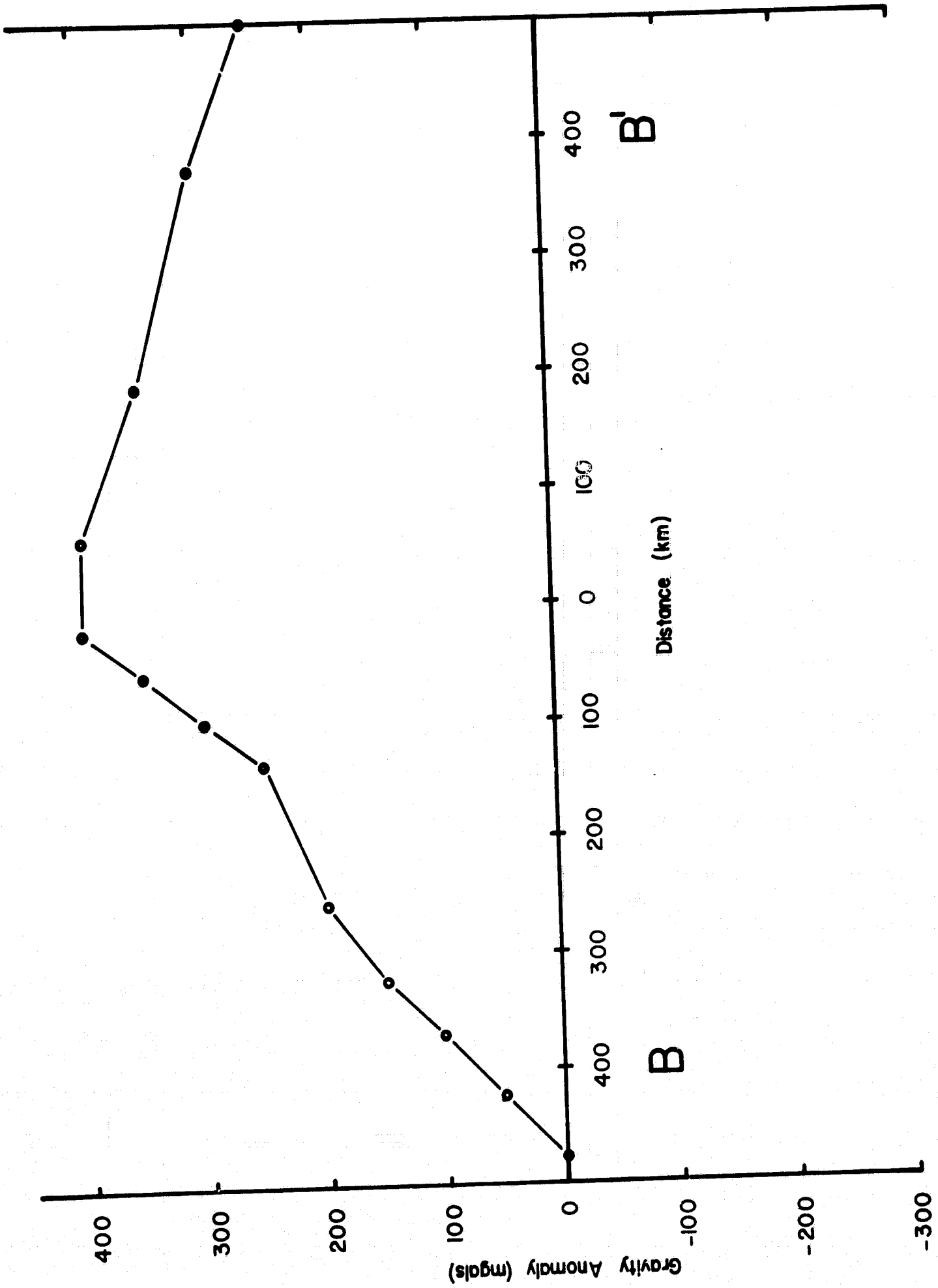


FIGURE 6 - North-South gravity anomaly profile across Mare Imbrium.

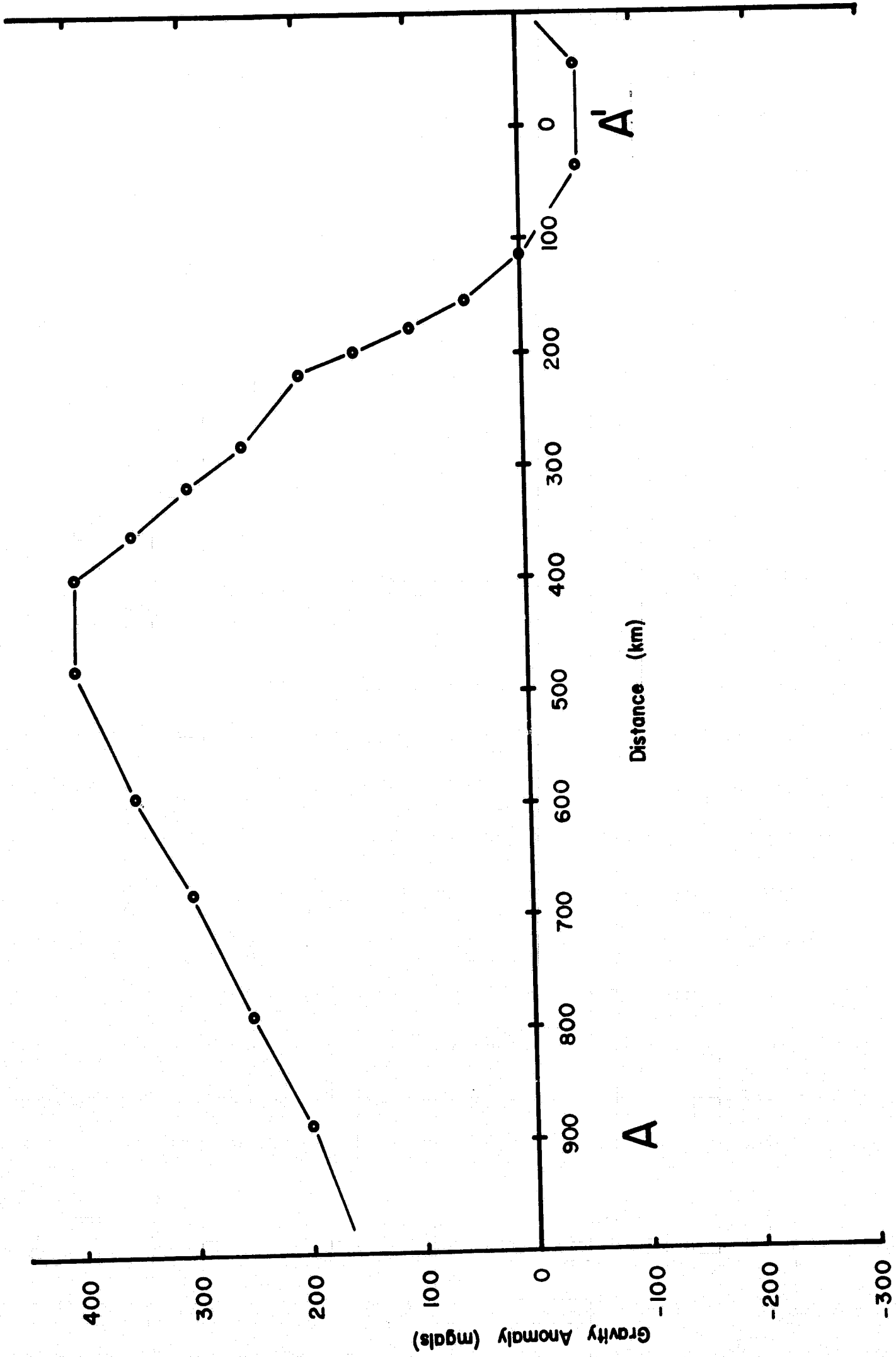


FIGURE 7 - East-West gravity anomaly profile across Mare Imbrium.

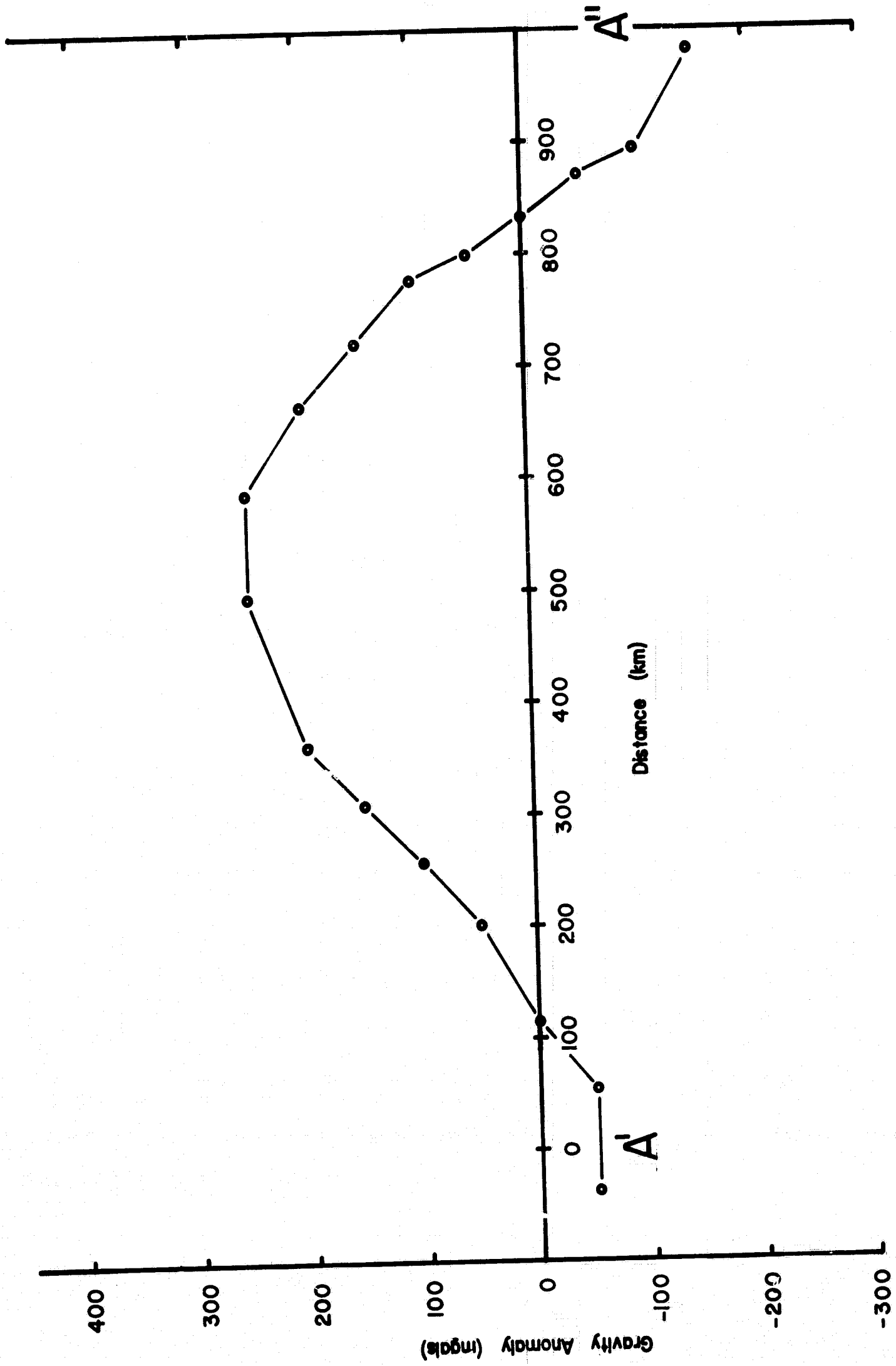


FIGURE 8 - East-West gravity anomaly profile across Mare Serenitatis.

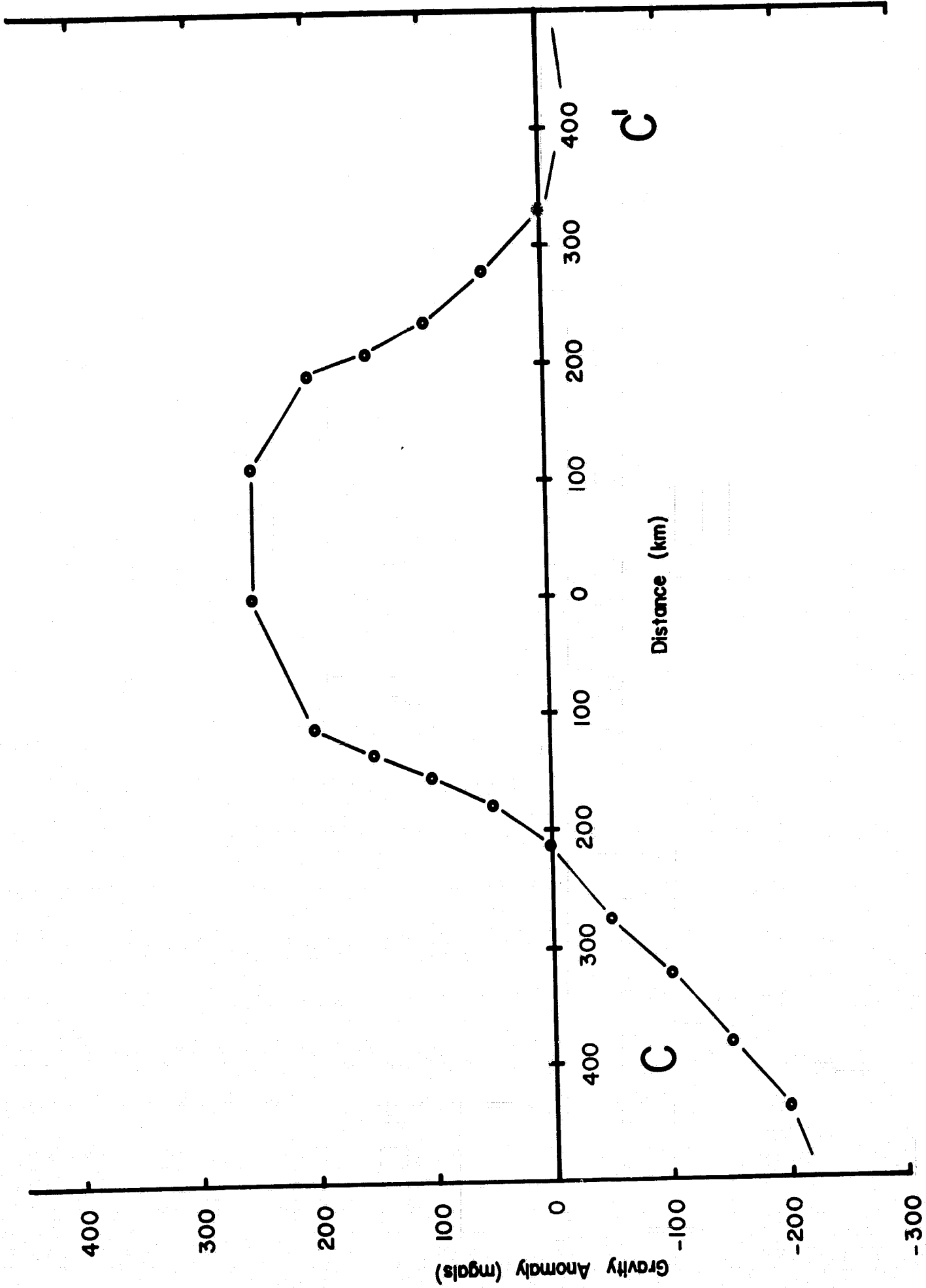


FIGURE 9. North-South gravity anomaly profile across Mare Serenitatis.

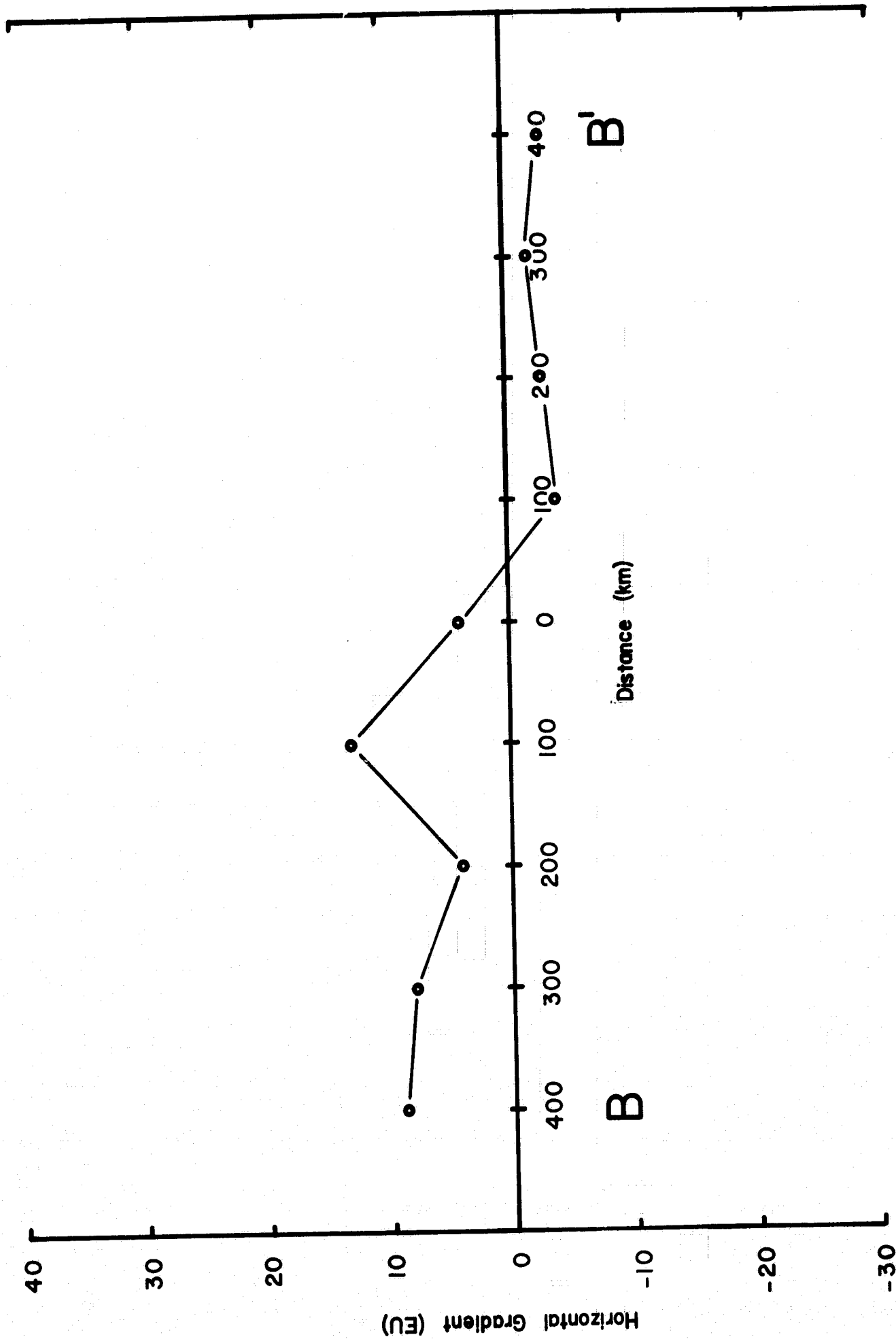


FIGURE 10. North-South horizontal gradient profile across Mare Imbrium.

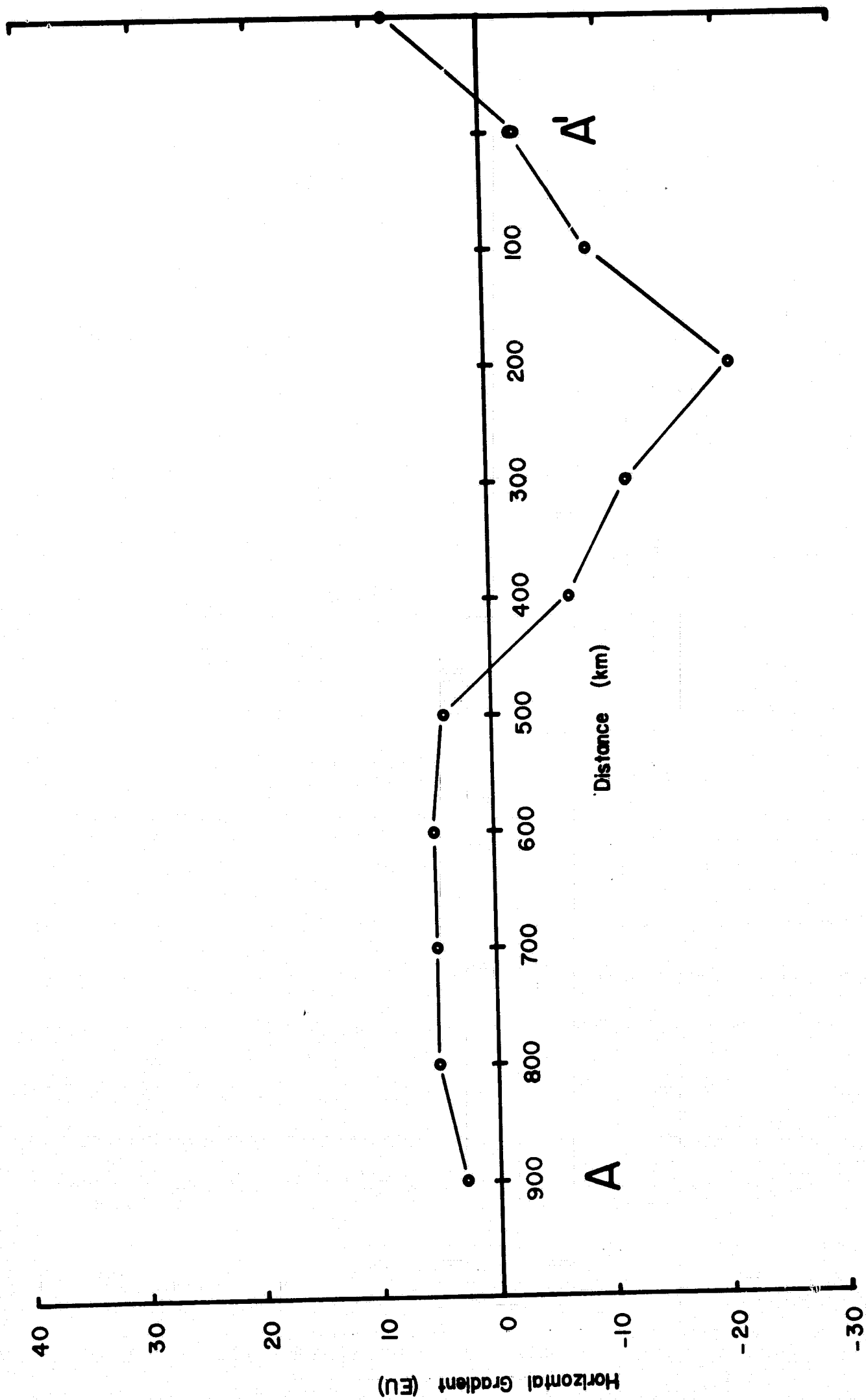


FIGURE 11. East-West horizontal gradient profile across Mare Imbrium.

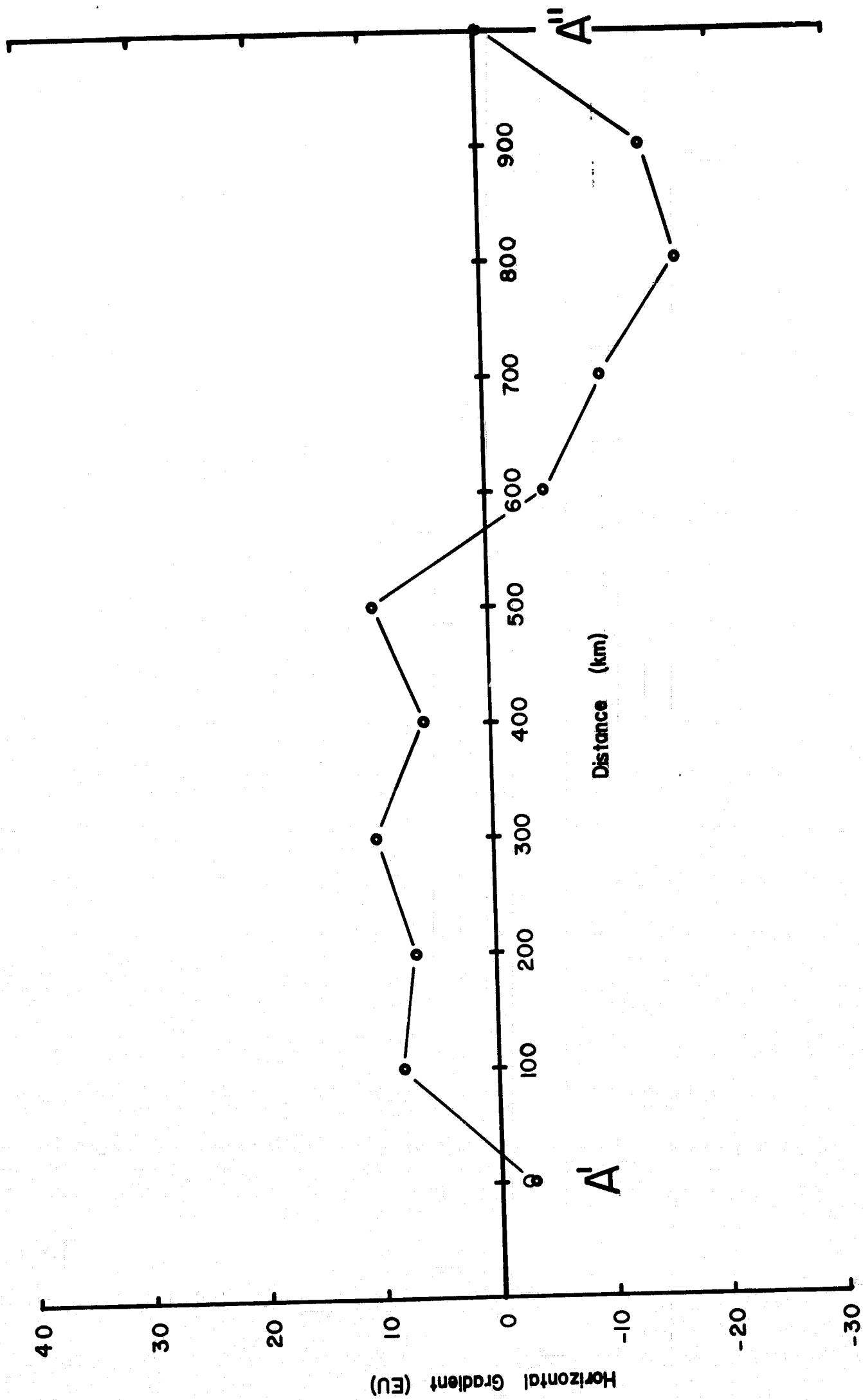


FIGURE 12 - East-West horizontal gradient profile across Mare Serenitatis.

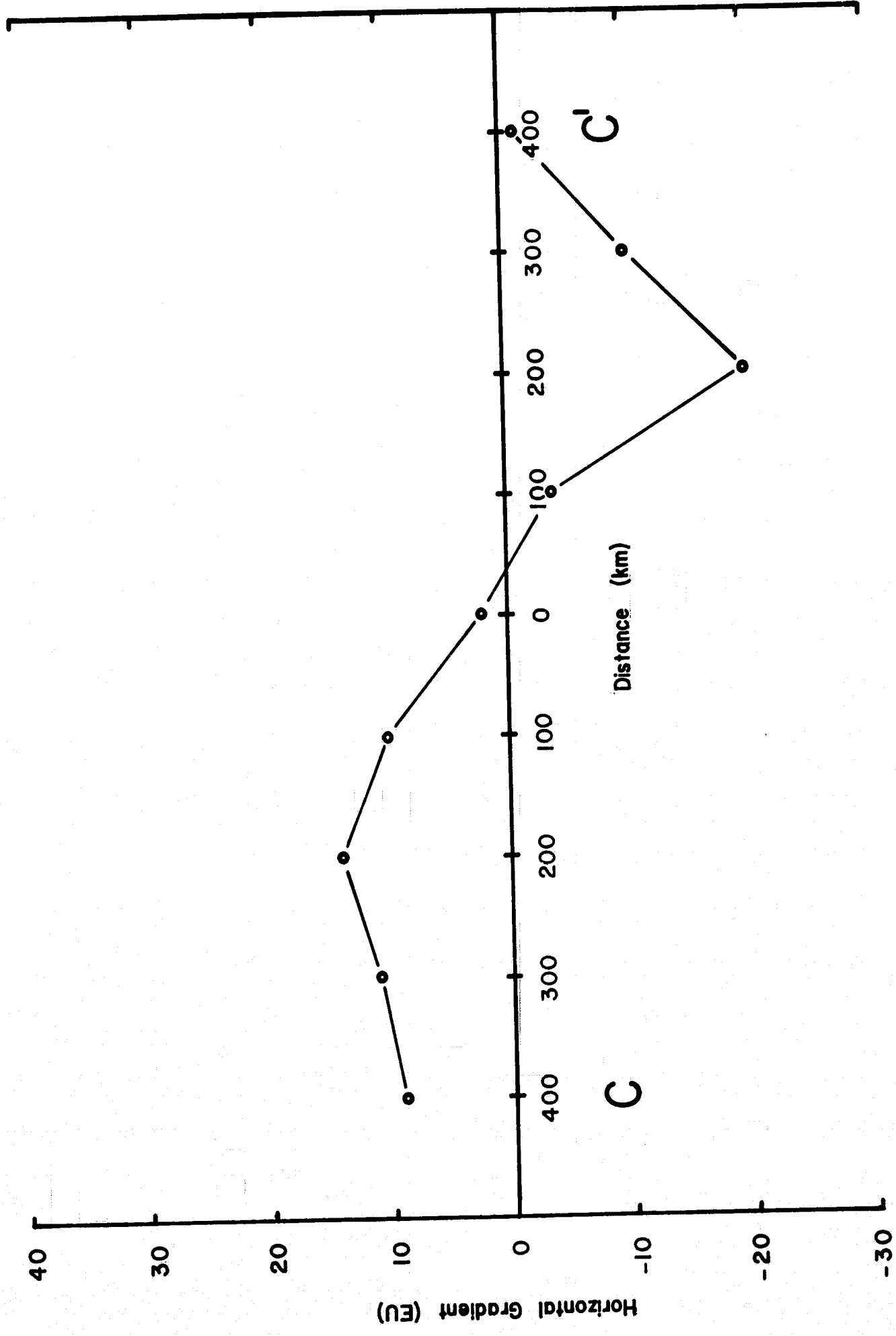


FIGURE 13. North-South horizontal gradient profile across Mare Serenitatis.

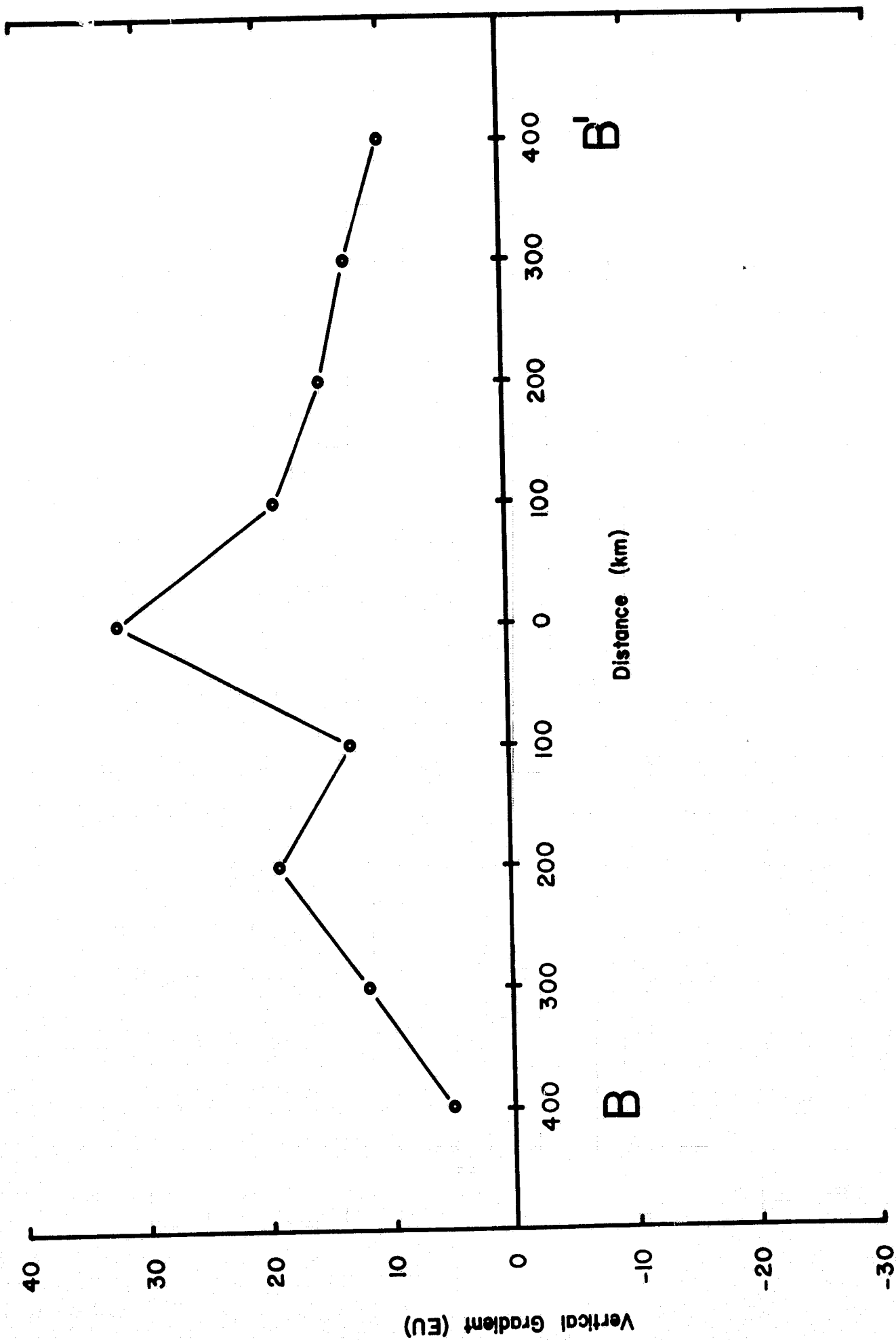


FIGURE 14. North-South vertical gradient profile across Mare Imbrium.

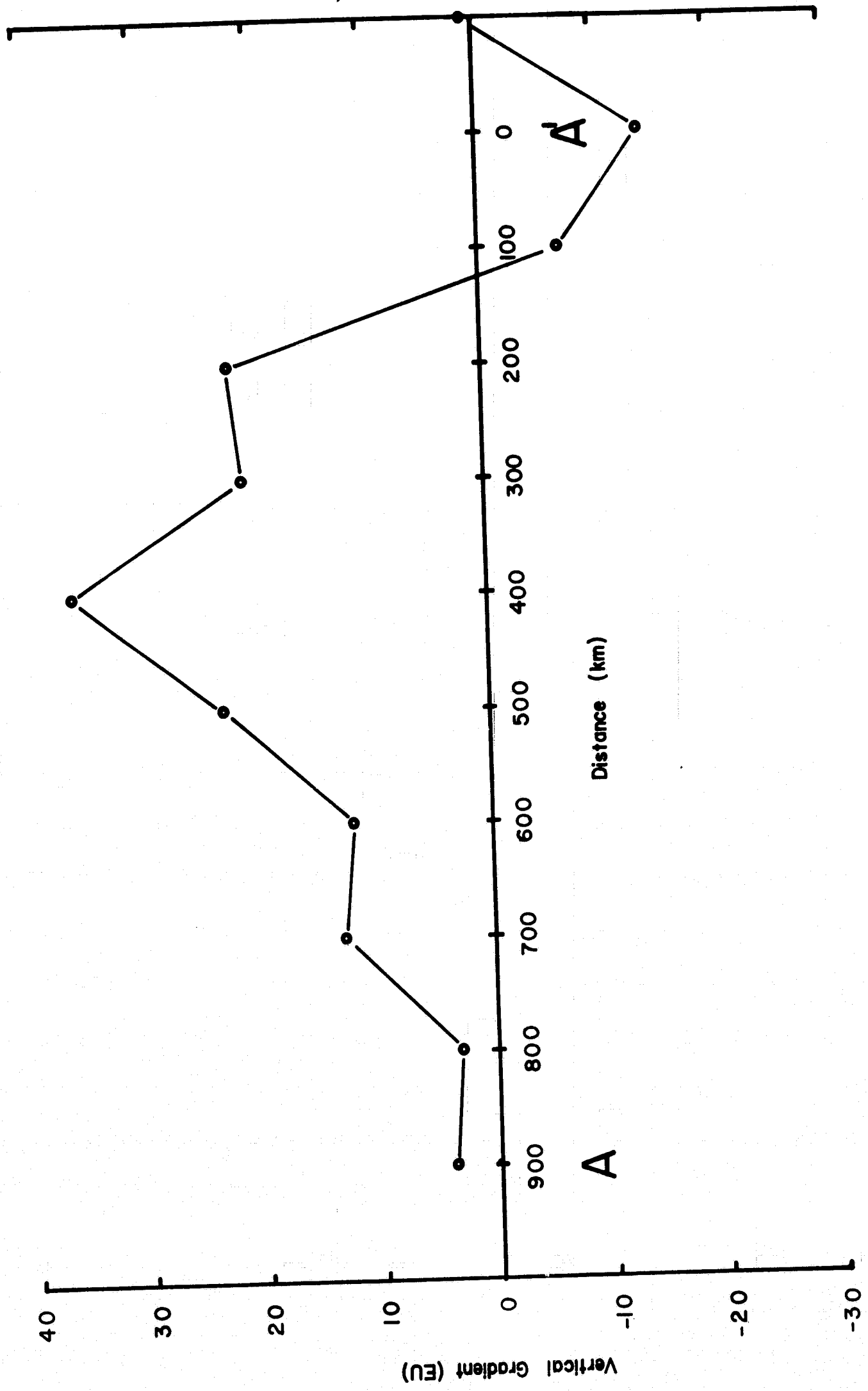


FIGURE 15. East-West vertical gradient profile across Mare Imbrium.

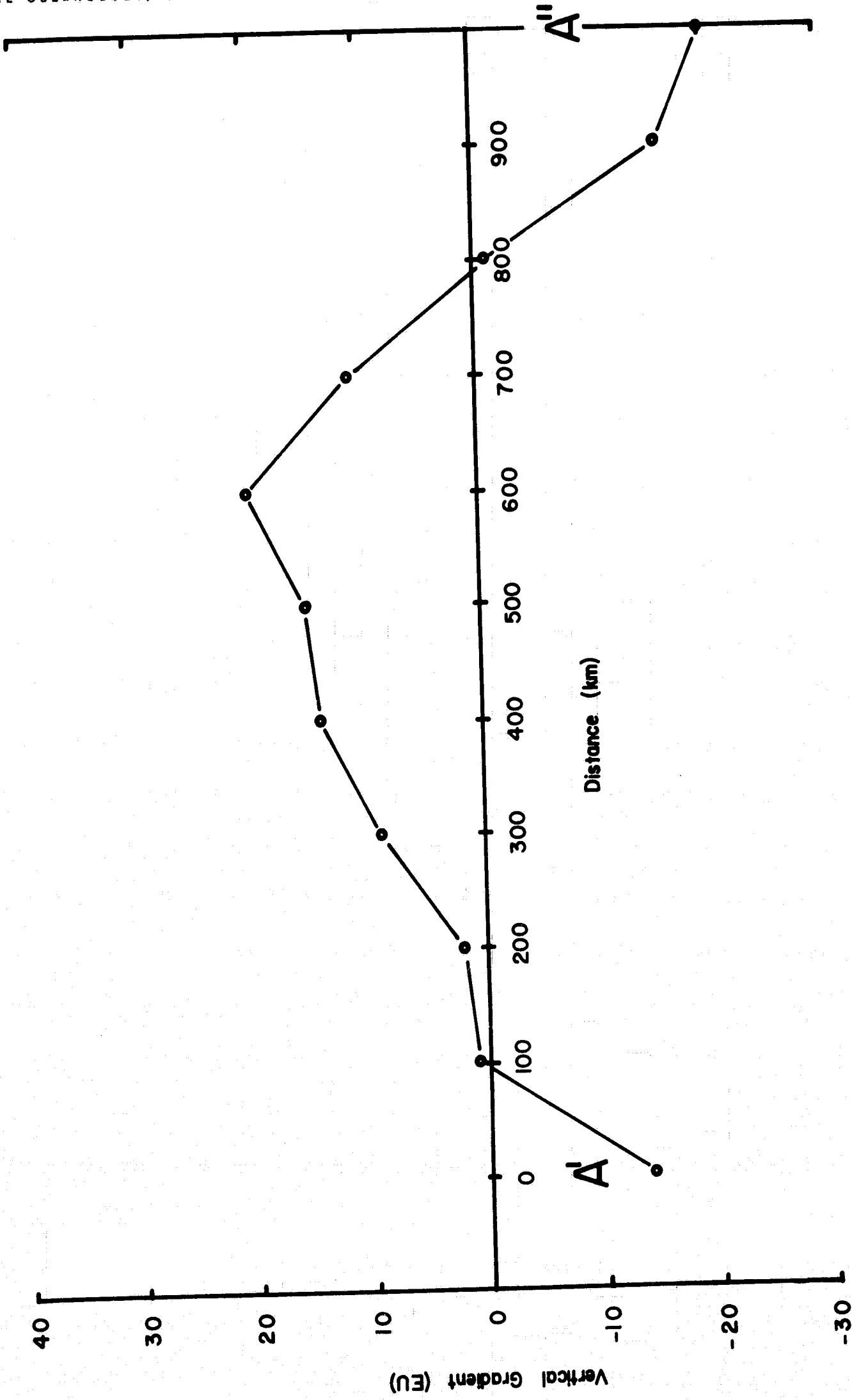


FIGURE 16. East-West vertical gradient profile across Mare Serenitatis.

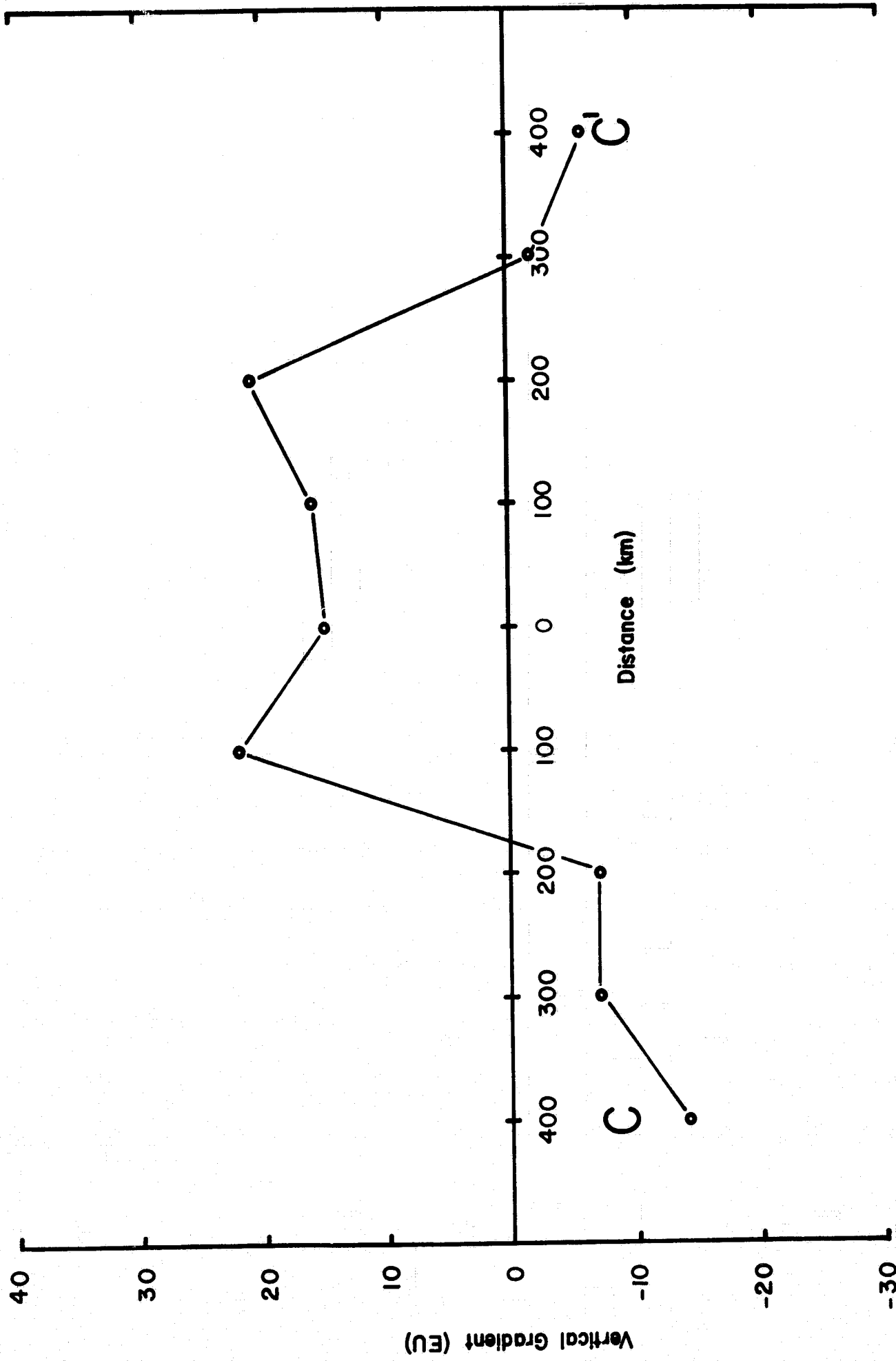


FIGURE 17. North-South vertical gradient profile across Mare Serenitatis.

V. MASCON INTERPRETATIONS

Most previous authors have modelled the Mascons as either spheres or discs of material.* Most of these have been based upon Free-Air anomalies which contain topographic effects and which could lead to uncertainties in interpretation. By using Bouguer anomalies and information contained in gravity gradient profiles, more light may be shed on the shape of the Mascons.

Gravity gradients in conjunction with the gravity anomalies aid in the geophysical interpretation of Mascons. For example, if we assume for the moment that the Mascon of Mare Imbrium is caused by a spherical mass, we can directly extract the depth of burial of the mass by using the peak values of the gravity anomaly and of the vertical gravity gradient. From Table 2 we know that the ratio of the maximum gravity anomaly to the maximum vertical gradient is equal to half the depth to the center of the mass. Using rough values for the profile B-B' across Mare Imbrium, we find:

$$\frac{Z}{2} = \frac{400 \text{ mgals}}{33 \text{ E.U.}} = \frac{4 \times 10^{-1} \text{ gals}}{3.3 \times 10^{-8} \text{ gals/cm}} = 1.2 \times 10^7 \text{ cm}$$

$$\text{or } \underline{\text{Depth}} = \underline{240 \text{ km}}$$

The corresponding mass estimate is about 3.5×10^{21} gms for a spherical body.

* Stipe, 1968; Conel and Holstrom, 1968; Baldwin, 1968; Urey, 1968; Campbell, O'Leary, and Sagan, 1969; Urey, 1969; Kane, 1969; Muller and Sjogren, 1969; Blackshear, 1969; Gottlieb and Laing, 1969; Wong, Buechler, Downs and Prislín, 1969; Lorell, 1969; Kane and Shoemaker, 1969; Wise and Yates, 1969; Gilvarry, 1969.

Further comparison of the gravity and gradient profiles of Mare Imbrium with the model curves of the sphere shown in Figure 1 reveals that the assumed spherical model is probably not correct. The Mascon gravity and gradient signatures of Mare Imbrium do not match the gravity and gradient signatures of the sphere even allowing for some uncertainty in the data. The vertical gradient signature of a flat disc is broader and flatter in relation to its height than is the signature of a sphere.

The unsuitability of the spherical model for Mare Serenitatis is obvious. The vertical gradient signature of Mare Serenitatis most closely resembles the gradient signature of a shallow disc (Figure 4). The vertical gradient profile C-C' (Figure 17) is particularly striking. The saddle-shaped central portion of the profile, which has steep sides falling to negative values, is characteristic of the vertical gradient profile over the center of a shallow disc. As the depth of the disc increases, the central depression gradually disappears and becomes a local maximum, the steep slope of the flank becomes more gradual, and the negative values of the gradient become more diffuse. The east-west vertical gradient profile of Mare Serenitatis (Figure 16) shows a broad signature whose maximum is not coincident with the center of the disc. The differences between the north-south and east-west profiles emphasize that the Mascon is not a perfectly symmetric disc-shaped structure, but is probably an irregular tabular structure with varying thickness.

VI. CONCLUSIONS

Because of the uncertainties and limitations of the data and the inherent limitations of the gradient approximation method, the gradient profiles are not precise measurements of the actual gradients. Nevertheless the gradient calculations are sufficiently accurate to support the following general conclusions:

1. The magnitudes of the vertical and horizontal gradient anomalies associated with features like the Mascons on the lunar surface are likely to be of the order of 10 to 40 E.U. Such anomalies are sufficiently large to be detected and defined by a gradiometer having one E.U. sensitivity or better, even at orbital altitudes.
2. The gradient profiles over Mares Imbrium and Serenitatis indicate that the most probable Mascon model is disc-or saucer-shaped.
3. Gravity gradients offer a supplementary or alternate technique for the mapping and interpretation of geologic structures.
4. More accurate gradient determinations from better gravity data or ideally from actual gradient measurements would greatly aid the interpretation of the lunar Mascons.

VII. RECOMMENDATIONS

This analysis was only preliminary in nature but in view of the information gained and the indicated potential of the gradient method, the following additional items of work are recommended:

1. Explore the application and utility of the gradient method in greater detail with consideration of other lunar Mascons and other lunar geologic structures.

2. Analyze the application and significance of orbital and lunar surface gradient measurements for mapping and interpreting anomalies in the lunar gravity field.

3. Perform a more detailed analysis and interpretation of Mascon gravity anomalies using more precise gravity data which will soon be available.

4. Prepare a more detailed and accurate Bouguer anomaly map of the moon by applying more rigorous and accurate terrain corrections to the gravity anomaly values. This map would aid in the accurate interpretation of Mascons.

5. Perform detailed model studies for the improved interpretation of Mascons using more elaborate model structures and computer programs.

6. Investigate other applications of the gradient technique including at least (a) tide-produced gravity gradients, (b) mass measurements of planetary satellites, asteroids and comets, and (c) planetary geodetic parameters.

ACKNOWLEDGMENTS

The contributions and discussions of William B. Chapman, Technical Monitor, are gratefully acknowledged.

REFERENCES

- Balavadze, B. K., The effect of topographic masses on the vertical component of the gravity gradient, Akad. Nauk. Gruzinskoy S.S.S.R. Soobshcheniya, 19, 30-32, 1957.
- Baranov, V., Interpretation des anomalies gravimetriques; quelques developpements recents, Bull. Geod., 45, 20-25, 1957.
- Baldwin, R. B., Lunar Mascons: Another interpretation, Science, 162, 1407-1408, 1968.
- Blackshear, W. T., Progress on lunar gravitational potential determination by analysis of Lunar Orbiter tracking data, (Abstract), Trans. Am. Geophys. Union, 50, 124, 1969.
- Campbell, M. J., B. T. O'Leary, and C. Sagan, Moon: Two new mascon basins, Science, 164, 1273-1275, 1969.
- Chinnery, M. A., Terrain corrections for airborne gravity gradient measurements, Geophysics, 26, 480-489, 1961.
- Conel, J. E. and G. B. Holstrom, Lunar Mascons: A near-surface interpretation, Science, 162, 1403-1405, 1968.
- Gilvarry, J. J., The nature of the lunar mascons (Abstract), Trans. Am. Geophys. Union, 50, 125, 1969.
- Gottlieb, P. and P. A. Laing, Mass distributions inferred from Lunar Orbiter tracking data (Abstract), Trans. Am. Geophys. Union, 50, 124, 1969.
- Grant, F. S. and G. F. West, Interpretation theory in applied geophysics, 584 pp., McGraw-Hill Book Company, New York, 1965.
- Kane, M. F., Doppler gravity, a new method, J. of Geophys. Res., 74, 6579-6582, 1969.

REFERENCES (Cont.)

Kane, M. F. and E. M. Shoemaker, Analysis of gravitational anomalies of the moon (Abstract), Trans. Am. Geophys. Union, 50, 125, 1969.

Lorell, J., The shape of the moon's gravity field as determined from the lunar orbiting tracking data (Abstract), Trans. Am. Geophys. Union, 50, 125, 1969.

Muller, P. M. and W. L. Sjogren, Mascons: Lunar mass concentrations, Science, 161, 680-684, 1968.

Muller, P. M. and W. L. Sjogren, A new reduction of lunar orbiter radio tracking data in describing the lunar near-side gravity field (Abstract), Trans. Am. Geophys. Union, 50, 124, 1969.

Nagy, Dezso, The evaluation of Heuman's lambda function and its application to calculate the gravitational effect of a right circular cylinder, Pure and Applied Geophysics, 62, 1965.

O'Keefe, J. A., Isostasy on the moon, Science, 162, 1405-1406, 1968.

Raspopov, O. M., Application of Numerov's formula in gravity exploration, Leningrad Univ., Uchenyye Zapiski, 249, 243-247, 1958.

Raspopov, O. M., The behavior of the vertical gradient of gravity in a mountainous region, Akad, Nauk. S.S.S.R. Izv, Ser. Geofiz., 8, 1231-1234, 1959.

Stipe, J. G., Iron meteorites as mascons, Science, 162, 1402-1403, 1968.

Talwani, M., J. L. Worzel, and M. Landisman, Rapid gravity computations for two-dimensional bodies with application to the Mendocino submarine fracture zone, J. Geophys. Res., 64, 49-59, 1959.

Urey, H. C., Mascons and the history of the moon, Science, 162, 1408-1410, 1968.

REFERENCES (Cont.)

Urey, H. C., The contending moons, Astronautics and Aeronautics,
7, 37-41, 1969.

Wise, D. U. and M. T. Yates, Mascons as structural relief
on a lunar Moho (Abstract), Trans. Am. Geophys. Union,
50, 125, 1969.

Wong, L., G. Buechler, W. D. Downs and R. H. Prislín,
Dynamical determination of mascons on the moon (Abstract),
Trans. Am. Geophys. Union, 50, 125, 1969.

APPENDIX A

A METHOD FOR COMPUTING THE GRAVITY AND
GRAVITY GRADIENT ANOMALIES FOR
TWO-DIMENSIONAL POLYGONS

```

C          GRAVITY ANOMALIES FOR 2-D POLYGONS
C          M. HOUSTON - 6/9/69
C THIS PROGRAM CALCULATES GRAVITY ANOMALIES ACCORDING TO THE
C SCHEME OF TALWANI, WORZEL, AND LANDISMAN (JGR, 64:49-59,1959)
C ALL DISTANCES ARE IN KILOMETERS, AND DENSITY CONTRASTS IN GM/CC
C THE PROGRAM REQUIRES POLYGONS AS TERRANE INPUT FROM A DATA FILE
C THE OPERATOR MAY INPUT EITHER INDIVIDUAL OBSERVATION POINTS
C OR SPECIFY A LIMITED NUMBER OF POINTS.
C UP TO TEN POLYGONS AND 375 OBSERVATION POINTS MAY BE USED

DIMENSION X(10,20),Z(10,20),N(10),RHO(10),IDATA(24),ARRAY(5,75,7)
COMMON PI,IVALUE
COMMON SUMX,SUMZ,XX,XX1,ZZ,ZZ1,THEI,THEI1
COMMON ANGLE,PHI,A,B,DUM,DUMMY

TYPE 163
CALL OPENW(3)
TYPE 169
169 FORMAT(/SINPUT FROM FILE $)
CALL OPENR(2)
TYPE 70
70 FORMAT(///)
PI = 3.1415926
AI = 0.0
IG = 0
IVALUE = 0
G = 6.67E-08
READ 2,107,IDATA
107 WRITE 3,107,IDATA
FORMAT(24A3/)
READ 2,100,NPOLY
WRITE 3,100,NPOLY
DO 1 I=1,NPOLY
READ 2,101,N(I),RHO(I)
WRITE 3,101,N(I),RHO(I)
NPTS = N(I)
DO 1 J=1,NPTS
READ 2,102,X(I,J),Z(I,J)
WRITE 3,102,X(I,J),Z(I,J)

C          N(I) = NUMBER OF POINTS IN ITH POLYGON
C          RHO(I) = DENSITY IN ITH POLYGON
C          DISTANCES ARE IN KILOMETERS

X(I,J) = X(I,J)*1.0E+05
Z(I,J) = Z(I,J)*1.0E+05
1 CONTINUE

100 FORMAT(I3/)
101 FORMAT(I4,F6.2/)
102 FORMAT(2F8.4/)
L=0
M=0
TYPE 164
164 FORMAT(/$CALCULATE GRADIENTS ? YES=1, NO=0 $)
ACCEPT 167,IGRAD
APE = FLOAT(IGRAD)
IF (IGRAD) 40,41,40
41 NT = 5
163 FORMAT(/$OUTPUT TO FILES/)
GO TO 51

```

```

40      NT = 7
51      TYPE 168
168     FORMAT(/$INPUT OBSERVATION POINTS, SERIES=1, INDIVIDUAL=0 S)
        ACCEPT 167,IND
167     FORMAT(I1/)
        IF (IND) 31,30,31
31      TYPE 162
162     FORMAT(/$Z-INITIAL OBSERVATION POINT,LIMIT,INCREMENTS/)
        ACCEPT 166,AZ,BZ,CZ
166     FORMAT(3F10.4)
        TYPE 165
165     FORMAT($X-INITIAL OBSERVATION POINT,LIMIT,INCREMENTS/)
        ACCEPT 166,AX,BX,CX
        GO TO 320
30      CONTINUE

20      TYPE 200
200     FORMAT(/$X COORDINATE, Z COORDINATES/)
        ACCEPT 103,XA1,ZA1
        IF (XA1-69.69) 50,53,50
50      L=1
        M=M+1
        GO TO 33
320     L=0
        ZA1 = AZ-CZ
32      ZA1 = ZA1 + CZ
        IF (ZA1-BZ) 53,601,601
601     L=L+1
        M=0
        XA1 = AX - CX
602     XA1 = XA1 + CX - (0.001)*APE
        IF (BX-XA1) 32,603,603
603     M=M+1
33      CONTINUE
        IG = 0
66      XA = XA1*1.0E+05
        IG = IG + 1
        ZA = ZA1*1.0E+05
        VS = 0.0
        HS = 0.0
        DO 2 I=1,NPOLY
        NPTS = N(I)
        X(I,NPTS+1) = X(I,1)
        Z(I,NPTS+1) = Z(I,1)
        SUMX = 0.0
        SUMZ = 0.0
        DO 3 J=1,NPTS
        XX = X(I,J) - XA
        ZZ = Z(I,J) - ZA
        XX1 = X(I,J+1) - XA
        ZZ1 = Z(I,J+1) - ZA
        IF (ZZ-ZZ1) 21,22,21
22      IF (ZZ) 23,24,23
24      SUMX = 0.0
        SUMZ = 0.0
        IVALUE = 0
        GO TO 99
23      CALL PR807
        IF (IVALUE) 24,97,24
97      SUMX = ZZ*ALOG(SIN(THEI1)/SIN(THEI))
        SUMZ = ZZ*(THEI1-THEI)
        GO TO 99
21      IF (XX-XX1) 34,26,34

```

```

26     IF (XX) 27,24,27
27     CALL PR807
      IF (IVALUE) 24,98,24
98     SUMX = XX*(THEI1-THEI)
      SUMZ = XX*(ALOG(COS(THEI)/COS(THEI1)))
      GO TO 99
34     CALL PR806
      IF (IVALUE) 24,99,24
99     CONTINUE
      VS = VS + SUMZ*RHO(I)
3     HS = HS + SUMX*RHO(I)
2     CONTINUE
      UZ1 = VS*G*(2000.0)
      UX1 = HS*G*(2000.0)
      R = SQRT(UZ1**2+UX1**2)
      ARRAY(L,M,1) = ZA1
      ARRAY(L,M,2) = XA1 - (0.001)*APE
      ARRAY(L,M,3) = UZ1
      ARRAY(L,M,4) = UX1
      ARRAY(L,M,5) = R
      GO TO (67,65,64),IGRAD+IG
65     UZ2 = UZ1
      UX2 = UX1
      XA1 = XA1 + 0.001
      GO TO 66
64     CONTINUE
      UXX = (UX1-UX2)*1.0E+04
      UZX = (UZ1-UZ2)*1.0E+04
      ARRAY(L,M,6) = UXX
      ARRAY(L,M,7) = UZX
67     IF (IND) 602,20,602

103    FORMAT(2F10.4)
53     WRITE 3,159
159    FORMAT(/3X$POSITIONS (KM)$9X$ANOMALIES (MGALS)$11X$GRADIENTS (EU)$)
      WRITE 3,158
158    FORMAT(/5X,$Z$,9X,$X$,8X,$UZ$,8X,$UX$,5X,$RESULTANTS,4X,$UZZ$,7X,$ZX
      DO 58 II=1,L
      DO 58 JJ=1,M
      WRITE 3, 157,(ARRAY(II,JJ,K),K=1,NT)
157    FORMAT(7(F8.2,2X)/)
58     CONTINUE
      CLOSE (3)
      TYPE 80
80     FORMAT(///$FINISS)
C     THIS IS THE END OF THE MAIN PROGRAM
      END

```

```

C          SUBROUTINE PR807
SUBROUTINE PR807
COMMON PI, IVALUE
COMMON SUMX, SUMZ, XX, XX1, ZZ, ZZ1, THEI, THEI1
COMMON ANGLE, PHI, A, B, DUM, DUMMY
A = ZZ
B = XX
CALL PR800
CALL PR808
IF (IVALUE) 2, 1, 2
1  THEI = ANGLE
A = ZZ1
B = XX1
CALL PR800
CALL PR808
IF (IVALUE) 2, 3, 2
3  THEI1 = ANGLE
A = ZZ1-ZZ
B = XX1-XX
CALL PR800
IF (IVALUE) 2, 4, 2
4  PHI = ANGLE
2  RETURN
END

```

```

C          SUBROUTINE PR806
SUBROUTINE PR806
COMMON PI, IVALUE
COMMON SUMX, SUMZ, XX, XX1, ZZ, ZZ1, THEI, THEI1
COMMON ANGLE, PHI, A, B, DUM, DUMMY
CALL PR807
IF (IVALUE) 45, 46, 45
46 IF (THEI-THEI1) 40, 41, 40
40 CONTINUE
AI = XX1+ZZ1*(XX1-XX)/(ZZ-ZZ1)
TANO = A/B
DUM = (COS(THEI)*SIN(PHI)/COS(PHI)-SIN(THEI))
DUM = ALOG(DUM/(COS(THEI1)*SIN(PHI)/COS(PHI)-SIN(THEI1)))
DUMMY = AI*SIN(PHI)*COS(PHI)
SUMZ = DUMMY*(THEI-THEI1+TANO*DUM)
SUMX = DUMMY*(TANO*(THEI1-THEI)+DUM)
GO TO 42
41 CONTINUE
SUMZ = 0.0
SUMX = 0.0
42 CONTINUE
45 RETURN
END

```

```

C          SUBROUTINE ARCTANGENT (PR800)
SUBROUTINE PR800
COMMON PI, IVALUE
COMMON SUMX, SUMZ, XX, XX1, ZZ, ZZ1, THEI, THEI1
COMMON ANGLE, PHI, A, B, DUM, DUMMY
IF (B) 900, 901, 900
901 ANGLE = PI/2.0
IF (A) 903, 907, 902
900 ANGLE = ATAN(A/B)
IF (A) 905, 905, 904
905 IF (B) 903, 902, 906
906 ANGLE = (2.0)*PI+ANGLE

```

```
GO TO 902
904 IF (B) 903,902,902
903 ANGLE = ANGLE+PI
GO TO 902
907 IVALUE = 1
902 CONTINUE
RETURN
END
```

```
C SUBROUTINE PR808
SUBROUTINE PR808
COMMON PI, IVALUE
COMMON SUMX, SUMZ, XX, XX1, ZZ, ZZ1, THEI, THEI1
COMMON ANGLE, PHI, A, B, DUM, DUMMY
IF (ANGLE-2.0*PI) 908,910,910
910 ANGLE = ANGLE-2.0*PI
908 CONTINUE
RETURN
END
```

APPENDIX B

DETERMINATION OF THE GRAVITY AND GRAVITY GRADIENT
ANOMALIES OVER A VERTICAL CYLINDER

Unlike solutions for the gravity field over simple shapes like a sphere or semi-infinite horizontal cylinder, the solution for the gravity field over a vertical cylinder is not a simple solution. The field is usually broken down into an infinite series of polynomials, each polynomial representing a gravity moment. To describe the field beyond the radius of the cylinder's largest dimension with sufficient accuracy usually requires only a few moments. Within this radius the higher moments become increasingly important and an increasing number of moments must be utilized to retain sufficient accuracy.

Several approximation methods were tried* but were found to be too crude an approximation for our models. We needed to investigate the gravity anomaly and gradients within several kilometers of the surface of a flat, thin vertical cylinder of hundreds of kilometers radius. It was decided to use the numerical approximation outlined below.

* Nagy, 1966; Grant and West, 1965.

The gravity field equation over a cylindrical ring is:

$$U_z = -G\rho \int_{Z_1}^{Z_2} \int_{R_1}^{R_2} \int_0^{2\pi} \frac{zr d\xi dr dz}{[\delta^2 + r^2 + z^2 - 2\delta r \cos\xi]^{3/2}}$$

- where
- G = gravitational constant
 - ρ = density contrast
 - Z = Z coordinate of the element
 - r = radius coordinate of the element
 - ξ = angular displacement of the element in the r, ξ plane
 - δ = radial displacement of the field observation point from the cylindrical axis
 - Z_2, Z_1 = upper and lower bounds of the cylindrical ring
 - R_2, R_1 = outer and inner bounds of the cylindrical ring

after integration in Z and R,

$$\begin{aligned}
 U_z = -G\rho \int_0^{2\pi} \left\{ \left[(r^2 - 2\delta r \cos \xi + \delta^2 + z_2^2)^{1/2} - (r^2 - 2\delta r \cos \xi + \delta^2 + z_1^2)^{1/2} \right. \right. \\
 + \delta \cos \xi \log 2 |r - \delta \cos \xi + (r^2 - 2\delta r \cos \xi + \delta^2 + z_2^2)^{1/2}| \\
 - \delta \cos \xi \log 2 |r - \delta \cos \xi + (r^2 - 2\delta r \cos \xi + \delta^2 + z_1^2)^{1/2}| \left. \right] \\
 - \left[(\delta^2 + z_2^2)^{1/2} - (\delta^2 + z_1^2)^{1/2} \right. \\
 + \delta \cos \xi \log 2 |(\delta^2 + z_2^2)^{1/2}| \\
 \left. \left. - \delta \cos \xi \log 2 |(\delta^2 + z_1^2)^{1/2}| \right] \right\} d\xi
 \end{aligned}$$

A computer program for an SDS-940 system has been written to numerically integrate the above equation. The program approximates the integral in double precision with a Simpson's rule numerical integration. The interval 0 to 2π must be divided into a number of integration steps (specified at run time) sufficient to achieve at least hundredth milligal accuracy everywhere above the cylinder. Gravity gradients are calculated by a finite difference method. For the vertical gradient the gravity anomaly is first calculated along a profile at a distance Z km above the cylinder, then gravity is recalculated at a height of $Z + 0.1$ km. A minimum of hundredth milligal accuracy ensures an accuracy of 1 E.U. for the gradients.


```

WRITE 3,106,DI,DLIM,DINC
106  FORMAT(/8HORIGLN =,F12.4,4X8HLIMIT =,F12.4,4X8HSTEP =,F12.4/)
WRITE 3,107
107  FORMAT(/17HDISPLACEMENT (KM),4X,23HGRAVITY ANOMALY (MGALS))

D = DI-DINC
4   D = D+DINC
IF (D-DLIM) 3,3,2
3   CONTINUE
PHI = DPHI
GFIELD = C(R1,0.)+C(R1,PI)-C(R0,0.)-C(R0,PI)
DO 1 J = 2,II,2
PHI1 = PHI + DPHI
GF1 = 4.0*(C(R1,PHI)-C(R0,PHI))
GF2 = 2.0*(C(R1,PHI1)-C(R0,PHI1))
PHI = PHI + DPHI + DPHI
GFIELD = GFIELD + GF1 + GF2
1   CONTINUE
GFIELD = DPHI*(GFIELD + 4.0*(C(R1,PHI)-C(R0,PHI)))/3.0
IF (D-0.0) 5,5.6
5   CONTINUE
C
C   GORDO IS THE THEORETICAL GRAVITY VALUE ON AXIS
C
GOFDO = PI*(Z1-Z0-SQRT(Z1*Z1+(R1-R0)*(R1-R0))
1+SQRT(Z0*Z0+(R1-R0)*(R1-R0)))
ERR = (GFIELD + GOFDO)*(2.0)*G*RHO
GFIELD = 2.0*G*RHO*GFIELD*(1.0)
WRITE 3,110,D,GFIELD,ERR
110  FORMAT(/2XF12.5,12XF12.5,10X,1PE15.6)
GO TO 4
6   CONTINUE
GFIELD = 2.0*G*RHO*GFIELD*(1.0)
WRITE 3,109,D,GFIELD
109  FORMAT(/2XF12.5,12X,F12.5)
GO TO 4
2   CONTINUE
CLOSE(2)
CLOSE(3)
STOP
END

```